HHS Public Access

Author manuscript

Cell Rep. Author manuscript; available in PMC 2024 November 13.

Published in final edited form as:

Cell Rep. 2024 February 27; 43(2): 113795. doi:10.1016/j.celrep.2024.113795.

The IRAK1/IRF5 axis initiates IL-12 response by dendritic cells and control of *Toxoplasma gondii* infection

Milton Pereira[1,*], **Theresa Ramalho**[2], **Warrison A. Andrade**[1], **Danielle F. Durso**[1], **Maria C. Souza**[1], **Katherine A. Fitzgerald**[1], **Douglas T. Golenbock**[1], **Neal Silverman**[1], **Ricardo T. Gazzinelli**[1,3,4,5,*]

[1]Division of Infectious Diseases and Immunology, Department of Medicine, University of Massachusetts Chan Medical School, Worcester, MA, USA

[2]Department of Molecular, Cell, and Cancer Biology, University of Massachusetts Chan Medical School, Worcester, MA, USA

[3]Centro de Tecnologia de Vacinas, Universidade Federal de Minas Gerais, Belo Horizonte, Minas Gerais, Brazil

[4]Instituto René Rachou, Fundaçaõ Oswaldo Cruz, Belo Horizonte, Minas Gerais, Brazil

[5]Lead contact

SUMMARY

Activation of endosomal Toll-like receptor (TLR) 7, TLR9, and TLR11/12 is a key event in the resistance against the parasite *Toxoplasma gondii.* Endosomal TLR engagement leads to expression of interleukin (IL)-12 via the myddosome, a protein complex containing MyD88 and IL-1 receptor-associated kinase (IRAK) 4 in addition to IRAK1 or IRAK2. In murine macrophages, IRAK2 is essential for IL-12 production via endosomal TLRs but, surprisingly, *Irak2*$^{-/-}$ mice are only slightly susceptible to *T. gondii* infection, similar to *Irak1*$^{-/-}$ mice. Here, we report that upon *T. gondii* infection IL-12 production by different cell populations requires either IRAK1 or IRAK2, with conventional dendritic cells (DCs) requiring IRAK1 and monocyte-derived DCs (MO-DCs) requiring IRAK2. In both populations, we identify interferon regulatory factor 5 as the main transcription factor driving the myddosome-dependent IL-12 production during *T. gondii* infection. Consistent with a redundant role of DCs and MO-DCs, mutations that affect IL-12 production in both cell populations show high susceptibility to infection *in vivo*.

In brief

*Correspondence: ricardo.gazzinelli@umassmed.edu (R.T.G.), milton.pereira@umassmed.edu (M.P.).

AUTHOR CONTRIBUTIONS

M.P., T.R., D.F.D., W.A.A., and M.C.S. performed the experiments. M.P., T.R., N.S., and R.T.G. designed the experiments. M.P., K.A.F., D.T.G., N.S., and R.T.G. analyzed and discussed the results. M.P., N.S., and R.T.G. wrote the manuscript. D.T.G., N.S., and R.T.G funded the project.

DECLARATION OF INTERESTS

The authors declare no competing interests.

SUPPLEMENTAL INFORMATION

Supplemental information can be found online at https://doi.org/10.1016/j.celrep.2024.113795.

By studying the impact of various IRAK deficiencies in *Toxoplasma gondii* infection, Pereira et al. demonstrate that IL-12 production involves activation of CNBP and IRF5 downstream of either IRAK1 or IRAK2, with DCs requiring IRAK1 and monocyte-derived DCs requiring IRAK2. These findings shed light on how IRAK redundancy occurs *in vivo*.

Graphical Abstract

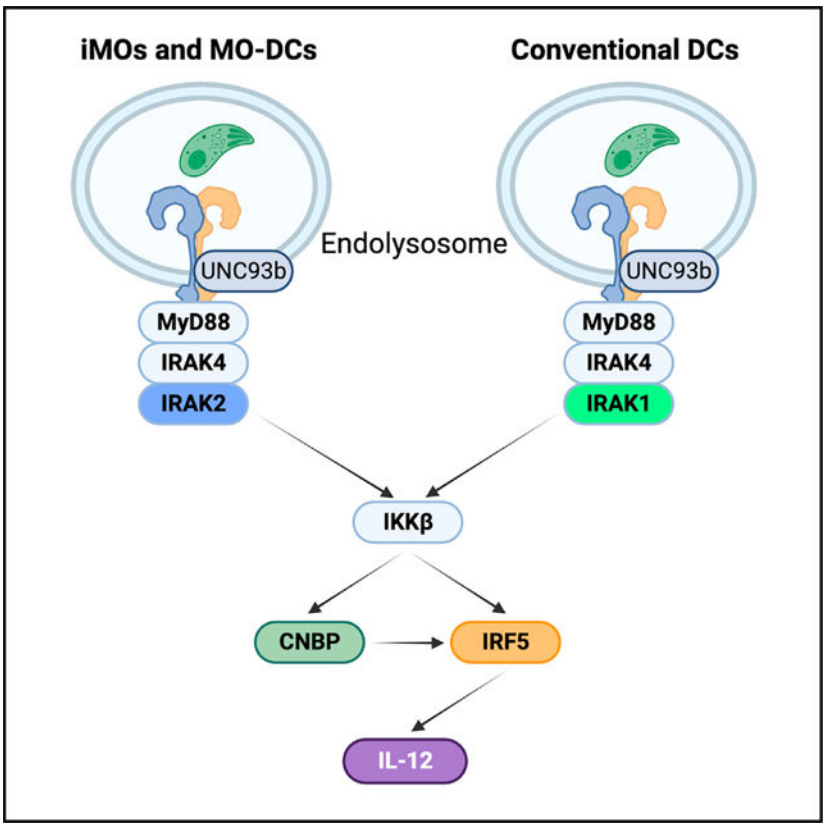

INTRODUCTION

The innate immune system is the first line of defense against invading microorganisms, and pattern recognition receptors (PRR), such as Toll-like receptors (TLRs), are at the center of this system. PRRs recognize conserved pathogen-associated molecular patterns (PAMPs), allowing cells to transduce signals into biologically relevant responses, such as production of cytokines and chemokines. TLRs are located in either the plasma membrane or endosomes (TLR3, TLR7, TLR9, TLR11, and TLR12), and signal transduction from TLRs require the adaptors Toll-interleukin receptor (TIR)-domain containing adaptor protein inducing interferon β (IFN-β) (TRIF) and/or myeloid differentiation primary response protein 88 (MyD88). TLR4 employs both adaptors, while TLR3 requires TRIF exclusively, and the remaining TLRs require MyD88.[1,2]

TLR engagement initiates the assembly of the myddosome, a supramolecular organizing center containing MyD88 and IL-1 receptor-associated kinase 4 (IRAK4) in addition to

IRAK1 and/or IRAK2.[2,3] IRAK1 and/or IRAK2 are required for activation of the E3 ubiquitin ligase tumor necrosis factor (TNF) receptor-associated factor 6 (TRAF6).[4,5] TRAF6 leads to production of pro-inflammatory cytokines, such as IL-12, via the IkB kinase (IKK) complex and activation of transcription factors such as activation protein 1 (AP-1) via mitogen-activated protein kinases (MAPKs), IFN regulatory factor 5 (IRF5), and the nuclear factor kB (NF-κB) protein c-Rel.[2,6] Interestingly, in lipopolysaccharide (LPS)-stimulated macrophages, c-Rel nuclear translocation and IL-12 transcription require cellular nucleic acid binding protein (CNBP), a DNA- and RNA-binding protein that is itself activated by the myddosome.[7,8]

Toxoplasma gondii is a ubiquitous protozoan that belongs to the phylum Apicomplexa and provides an interesting example of parasite-host coadaptation and successful transmission in nature.[9] As a result of being a natural intermediate host, the rodent immune system evolved to effectively cope with *T. gondii* infection.[10] Hence, in addition to its medical relevance, mice infected with *T. gondii* are an excellent model to study the mechanisms of host defense against intracellular pathogens.[11] Additionally, *T. gondii* is an invaluable tool to study the function of endosomal TLRs that signal via MyD88, as mouse resistance to acute infection with this parasite is primarily mediated by TLR7, TLR9, and TLR11/12.[11] In this model, upon TLR activation, IL-12 is produced by key cell populations, such as conventional $CD11c^+$ dendritic cells (DCs), $CD11b^+$ inflammatory monocytes (iMOs), and $CD11b^+$ monocyte-derived DCs (MO-DCs).[12–15] IL-12, in turn, triggers natural killer (NK) and T lymphocytes to produce IFN-γ.[16,17] Therefore, the IL-12/IFN-γ axis is central for the resistance to *T. gondii* infection.[10,11]

Mice deficient in MyD88 or UNC93b, a trafficking chaperone for endosomal TLRs,[18–21] die in the first days of infection with *T. gondii*, a consequence of low IL-12 production.[22–24] TLR11 and TLR12 are endosomal TLRs and function as a heterodimeric pair highly specific for *T. gondii* profilin-like protein (TgPLP).[25] In comparison with the MyD88 knockouts (KOs) and UNC93b mutants, infected TLR11 or TLR12 KO mice show a moderate increase in parasitism and no lethality.[23,25,26] Nevertheless, mice with combined deletion of the endosomal *Tlr11*, *Tlr7*, and *Tlr9* genes are as susceptible to *T. gondii* as the MyD88 KO and the UNC93b mutants,[26] demonstrating a redundancy between TgPLP and RNA and DNA sensing by these endosomal TLRs.

Like MyD88, IRAK4 is essential for TLR function.[27–29] IRAK4 KO mice are thought to phenocopy MyD88 KO mice and are highly susceptible to viral, bacterial, fungal, and parasitic infections.[30] Importantly, IRAK4 KO mice are greatly susceptible to *T. gondii* infection due to deficient IL-12 production.[31] After engagement of endosomal TLRs and myddosome formation, little is known about the signaling events that culminate in IL-12 transcription in the context of *T. gondii* infection. For instance, in macrophages stimulated with LPS, the transcription factor c-Rel is essential for IL-12 expression.[32] However, c-Rel is not required for IL-12 production upon *T. gondii* infection *in vivo*, and c-Rel-deficient DCs produce similar amounts of IL-12.[33] Thus, the transcription factor responsible for IL-12 production upon *T. gondii* infection remains elusive. Additionally, the roles of IRAK1 and IRAK2 require further elucidation, as these kinases are not redundant in every context.[3] For instance, efficient cytokine production in murine macrophages require IRAK2,[27,34] whereas

mouse embryonic fibroblasts require IRAK1.[35] Finally, CNBP KO mice are partially susceptible to *T. gondii* infection and have impaired IL-12 production, but it is presently unknown how CNBP controls IL-12 in *T. gondii*-exposed DCs.[8]

Here, we report that IRAK1-dependent activation of CNBP and IRF5 is a key signaling event required for IL-12 release elicited by *T. gondii* infection of DCs. Importantly, compared with macrophages and monocytes, our data indicate a differential requirement of IRAKs for IL-12 production by conventional $CD11c^+$ DCs exposed to *T. gondii* tachyzoites and other TLR ligands. Macrophages and MO-DCs require IRAK2 for IL-12 production,[27] but surprisingly, we observed that *Irak2*$^{-/-}$ mice are only slightly more susceptible to *T. gondii* infection, similar to *Irak1*$^{-/-}$ mice. Mechanistically, IRAK2 deficiency does not impair IL-12 release from $CD11c^+$ DCs, but IRAK1 deficiency does. In murine macrophages, the IRAK4 kinase activity is required for IL-12 production via endosomal TLRs,[34,36,37] but this is not essential in $CD11c^+$ DCs, and downstream IRAK1 can partially compensate for the loss of IRAK4 kinase activity. Accordingly, mice expressing a kinase-dead IRAK4 are partially susceptible to *T. gondii* infection. IRAK4 KO and IRAK1/2 double KO mice are highly susceptible to infection, as these mutations completely block IL-12 production in both $CD11b^+$ and $CD11c^+$ cells. We found that these deficiencies in IL-12 production correlated with deficient IRF5 activation. Indeed, IRF5 KO mice showed great susceptibility to *T. gondii* infection *in vivo*, and *Irf5*$^{-/-}$ $CD11c^+$ DCs and splenic $CD11b^+$ cells exposed to *T. gondii* fail to produce IL-12. Hence, we identify the IRAK1/IRF5 axis as a key mediator of host resistance to *T. gondii* infection through its role in regulating cytokine induction in $CD11c^+$ DCs.

RESULTS

IRAKs control primary infection with *T. gondii*

While there is a MyD88-independent pathway that mediates resistance to highly attenuated *T. gondii* strains,[38,39] the canonical pathway of host immunity to virulent natural *T. gondii* strains involves the endosomal TLRs MyD88 and IRAK4.[22,26,31] Here, we sought to evaluate how different IRAK proteins contribute to host resistance to *T. gondii* using a model of intraperitoneal (i.p.) infection with cysts of *T. gondii* strain Me49. We confirm that *Irak4*$^{-/-}$ mice are highly susceptible to *T. gondii*, showing 100% mortality by 30 days post infection (Figure 1A). In contrast, the single IRAK1 or IRAK2 KO mice survived the infection like wild-type (WT) animals but showed a significant increase in the number of cysts in the brain (Figure 1B). This was a surprising observation, as previous studies suggested an essential role of IRAK2 in IL-12 production, while IRAK1 was dispensable;[27,34] therefore, we expected that *Irak2*$^{-/-}$ mice would phenocopy *Irak4*$^{-/-}$ and that *Irak1*$^{-/-}$ mice would behave like WT animals. The double IRAK1/IRAK2 KO mice were as susceptible as the *Irak4*$^{-/-}$ mice, consistent with the idea that IRAK1 and IRAK2 can compensate for each other (Figure 1A). The levels of circulating IL-12 p40, an indicator of the levels IL-12, and IFN-γ in plasma (Figures 1D and 1E) as well as produced *in vivo* in the peritoneal cavity (Figures 1F and 1G) suggests that IRAK1 and IRAK2 are redundant *in vivo*, which is further corroborated by the fact that IRAK1/IRAK2 double KO animals are severely deficient in cytokine production.

To further investigate the role of IRAK4 in this response, we performed infection assays in mice with a mutant IRAK4 knocked in (*Irak4* Ki), containing two point mutations in the IRAK4 kinase domain (lysine-to-methionine point mutations at positions 213 and 214), which silences its kinase activity.[37] We expected that *Irak4* Ki animals would be as susceptible to infection as *Irak4*$^{-/-}$ mice, as prior studies reported that *Irak4* Ki and *Irak4*$^{-/-}$ cells completely fail to produce cytokines in response to endosomal TLR agonists.[34,37,40,41] Surprisingly, *Irak4* Ki mice showed an intermediate resistance between WT and *Irak4*$^{-/-}$ ($p < 0.001$ in comparison with the WT, $p < 0.0001$ in comparison with *Irak4*$^{-/-}$, log rank test), with around half of the animals succumbing after 30 days post infection and nearly 90% of them succumbing by day 40 post infection (Figure 1C). Moreover, we demonstrated that *Irak4* Ki mice crossed with either the *Irak1*$^{-/-}$ or *Irak2*$^{-/-}$ mice were as susceptible to *T. gondii* infection as *Irak4*$^{-/-}$ mice (Figure 1C) ($p > 0.05$, log rank test). Similarly, defects in IRAK4 significantly impacted the production of IL-12 and IFN-γ, with *Irak4*$^{-/-}$ animals (lacking IRAK4 scaffold function) showing more severe deficiencies than animals containing a kinase-deficient IRAK4 scaffold (*Irak4* Ki) (Figures 1D–1G).

Ex vivo, splenocytes exposed to *T. gondii* tachyzoites produced IL-12 independent of IRAK2 but partially required IRAK1 and IRAK4 kinase activity. *Irak1*$^{-/-}$*Irak4* Ki splenocytes also showed less IL-12 production in comparison with *Irak4* Ki splenocytes —further evidence that IRAK1 might compensate for the loss of IRAK4 kinase activity (Figure 1H). In this population, CD11c^{+} DCs are the main source of IL-12.[12] However, pre-treatment of splenocytes with IFN-γ for 24 h, followed by exposure *to T. gondii*, led to similar IL-12 output in *Irak1*$^{-/-}$, *Irak2*$^{-/-}$, and WT cells. Likewise, priming with IFN-γ partially restored the production of *T. gondii*-induced IL-12 release by splenocytes from *Irak1*$^{-/-}$*Irak4* Ki mice (Figure 1I). In both IFN-γ-primed and unprimed splenocytes, *Irak4*$^{-/-}$ and *Irak1*$^{-/-}$*Irak2*$^{-/-}$ cells failed to produce IL-12 (Figures 1H and 1I). Since treatment of splenocytes with IFN-γ increases the CD11b^{+} population (MO-DCs and iMOs) (Figure S1),[42] we speculated that different cell populations preferentially employ IRAK1 or IRAK2 in the myddosome.

IRAK1 is required for IL-12 production in DCs

Considering what is known regarding MyD88 and IRAK4 in host resistance to *T. gondii* infection,[22,31] we assumed that the primary role of IRAKs in response to *T. gondii* is in IL-12 production by iMOs, MO-DCs, and/or DCs, the main sources of IL-12 *in vivo*.[13–15] Thus, the low levels of IFN-γ observed in the peritoneal cavity and plasma of *Irak1*$^{-/-}$*Irak2*$^{-/-}$, *Irak4*$^{-/-}$, and the various *Irak4* Ki mice are a consequence of the impaired IL-12 released by these antigen-presenting cells. Hence, we evaluated the levels of IL-12 produced by splenic CD11b^{+} cells (consisting of iMOs and MO-DCs) as well as CD11c^{+} DCs stimulated with R848 (a TLR7 agonist) or *T. gondii* tachyzoites. Bone marrow-derived macrophages (BMDMs) were also included, as the role of IRAK proteins is better understood in this cell type.[34] In BMDMs or CD11b^{+} cells stimulated with either R848 or *T. gondii*, IRAK1 deficiency did not inhibit IL-12 production, whereas IRAK2 deficiency did, and is essential in the case of R848-stimulated BMDMs (Figures 2A, 2B, 2D, and 2E). Surprisingly, IRAK1 is more important than IRAK2 for IL-12 production in CD11c^{+} DCs exposed to *T. gondii* and R848 (Figures 2C and 2F).

To understand why different cell populations primarily require either IRAK1 or IRAK2, we investigated the expression levels of these myddosome components in different cell types. Under unstimulated conditions, we found similar expression levels of MyD88 and IRAK4 in BMDM and $CD11b^+$ and $CD11c^+$ cell populations, whereas IRAK2 was expressed at higher levels in BMDMs and $CD11b^+$ cells, and IRAK1 was expressed at higher levels in $CD11c^+$ DCs (Figures 2G, 2H, S2A, and S2B), corroborating the observations that IRAK1 is more important in $CD11c^+$ DCs, while IRAK2 is more relevant in BMDMs and $CD11b^+$ cells. Since TLR/IL-1R stimulation leads to IRAK1 degradation and IRAK2 upregulation,[5,36,43–45] we investigated whether these events follow different patterns in $CD11b^+$ and $CD11c^+$ cells. For this, splenic $CD11b^+$ cells and $CD11c^+$ DCs were exposed to *T. gondii* for up to 24 h, and the whole-cell lysates were treated with phosphatase and deubiquitinase (as these post-translational modifications might decrease the binding of the primary antibody used for immunoblotting), and IRAK1 and IRAK2 were probed by immunoblotting. In these *T. gondii*-exposed populations, IRAK1 and IRAK2 showed similar behavior, with the IRAK1 protein quickly disappearing and IRAK2 expression levels increasing (Figures 2I and S2C). Importantly, the expression and behavior of IRAK1 and IRAK2 are independent from one another (Figures 2J and S2D).

Consistent with the *ex vivo* data shown in Figures 1F and 1G, the levels of IL-12 produced by splenic $CD11b^+$ cells and $CD11c^+$ DCs exposed to either *T. gondii* or R848 from *Irak1*$^{-/-}$*Irak2*$^{-/-}$, *Irak4*$^{-/-}$, and *Irak4* Ki mice were very low. Interestingly, the production of IL-12 by *Irak4*$^{-/-}$ $CD11c^+$ DCs was close to absent, while *Irak4* Ki DCs produced reduced but still detectable levels of IL-12. We reasoned that this residual production involves the IRAK4 scaffold and either IRAK1 or IRAK2. To test this hypothesis, we stimulated *Irak4* Ki, *Irak1*$^{-/-}$*Irak4* Ki, and *Irak2*$^{-/-}$*Irak4* Ki DCs with R848 or *T. gondii* and found that IRAK1 can partially compensate for loss of IRAK4 kinase activity, as *Irak1*$^{-/-}$*Irak4* Ki DCs failed to produce IL-12, while IRAK2 had a minimal effect with *T. gondii* challenge (Figures 2K and 2L).

These data demonstrate that DCs require IRAK1 and partially require IRAK4 kinase activity for IL-12 production upon *T. gondii* infection. In contrast, $CD11b^+$ cells behave like BMDMs, which require IRAK2 and IRAK4 kinase activity to induce IL-12 production.[34]

MAPK and NF-κB activation requires IRAK4 kinase activity, while IRAK1 and IRAK2 are redundant

Since $CD11c^+$ DCs can be obtained in high numbers and produce the highest levels of IL-12 p40 when exposed to *T. gondii* (Figures 2D–2F), we decided to focus our study on how IRAK1 impacts signaling that leads to IL-12 production in $CD11c^+$ DCs exposed to *T. gondii*. Under resting conditions, members of the NF-κB family are kept in the cytosol due to interactions with NF-κB inhibitor alpha (IκB-α). Upon myddosome activation, IκBα is phosphorylated and K48 is ubiquitinated and degraded, allowing NF-κB proteins such as RelA and c-Rel to translocate to the nuclei; in addition, these NF-κB proteins are phosphorylated upon activation.[6,46] In R848-stimulated BMDMs, NF-κB activation requires IRAK4 kinase activity and either IRAK1 or IRAK2.[27,34] Similarly, DCs exposed to *T. gondii* or stimulated with R848 show redundancy between IRAK1 and IRAK2, as IkBa

and RelA phosphorylation, IkBa degradation, and nuclear translocation of RelA and c-Rel (readouts of NF-κB activation) were similar between the WT and either single IRAK KO. However, *Irak1*$^{-/-}$*Irak2*$^{-/-}$ CD11c^{+} DCs failed to activate NF-κB (Figures S3, S4, and 3A–3D). Similar patterns are observed in phosphorylation of MAPKs p38, extracellular signal-regulated kinase (ERK), and c-Jun N-terminal kinase (JNK) (a readout of their activation), with IRAK1 and IRAK2 showing redundancy (Figure 3E). On the other hand, IRAK4 kinase activity was essential for both NF-κB and MAPK activation (Figures 3B 3D, and 3F).

Hence, the patterns of NF-κB and MAPK activation in DCs are similar to BMDMs[34] and do not correlate with IL-12 production in response to *T. gondii* challenge. *Irak1*$^{-/-}$ DCs are not deficient in NF-κB and MAPK activation but are deficient in IL-12 production. Conversely, *Irak4* Ki DCs are completely impaired in NF-κB and MAPK activation but still produce detectable amounts of IL-12 (Figures 2 and 3). This is consistent with prior observations that NF-κB is not essential for IL-12 induction in conventional DCs upon *T. gondii* infection.[33]

IRAK1-mediated IRF5 activation drives IL-12 production in *T. gondii*-exposed DCs

Our data (Figure 3) and prior studies indicate that members of the NF-κB family are not responsible for IL-12 production in DCs.[33] Previously, it has been demonstrated that the transcription factor IRF5 drives pro-inflammatory responses downstream of endosomal TLR activation.[47–50] However, links between IRF5 and *T. gondii* infection are unknown. Hence, we evaluated IRF5 activation by measuring its nuclear translocation in CD11c^{+} DCs exposed to *T. gondii*.

In CD11c^{+} DCs, exposure to *T. gondii* for 2 h drives IRF5 nuclear translocation (Figures S5A and S5B), and largely requires IRAK1 (Figures 4A and S5C). Interestingly, a small amount of IRF5 nuclear translocation is observed in *Irak1*$^{-/-}$ and is completely absent in *Irak1*$^{-/-}$*Irak2*$^{-/-}$ DCs. This suggests that, while IRAK1 is primarily responsible for driving IRF5 activation, IRAK2 may still play a secondary role. IRAK4 is essential for IRF5 nuclear translocation, but loss of its kinase activity only partially impaired IRF5 activation. This residual IRF5 activation requires IRAK1 and not IRAK2, as *Irak1*$^{-/-}$*Irak4* Ki showed no IRF5 activation, while *Irak2*$^{-/-}$*Irak4* Ki behaved like *Irak4* Ki DCs (Figures 4D and S5D). In splenic CD11b^{+} cells, IRAK2 and the kinase activity of IRAK4 were completely required for IRF5 nuclear translocation upon exposure to *T. gondii* (Figures 4C and S5E). These IRF5 nuclear translocation results nicely correlate with the IL-12 response observed in *T. gondii*-exposed DCs and CD11b^{+} cells (Figure 2).

To unambiguously link IRF5 to IL-12 production in response to *T. gondii*, we obtained BMDMs and CD11b^{+} and CD11c^{+} cells from WT and *Irf5*$^{-/-}$ mice, exposed these cells to R848 or *T. gondii* tachyzoites, and quantified IL-12 p40 in the culture supernatants. While *Irf5*$^{-/-}$ BMDMs and CD11b^{+} cells showed a partial reduction in IL-12 production, IRF5 deletion in CD11c^{+} DCs nearly completely prevented the production of this cytokine (Figures 4D–4F). Accordingly, chromatin immunoprecipitation (ChIP) assays using anti-IRF5 revealed an enrichment of the *Il12b* promoter in WT DCs exposed to *T. gondii* tachyzoites (Figure 4G)—further evidence that IRF5 directly controls *Il12b* transcription in CD11c^{+} DCs. The dramatic reduction in IL-12 output observed in *Irf5*$^{-/-}$ CD11c^{+} DCs in comparison with *Irf5*$^{-/-}$ CD11b^{+} and BMDMs is of note, and while the reasons for these

differences are likely multifactorial, we speculated that different IRF5 expression levels in these cell types could account for some of these differences. IRF5 is a transcription factor that is not ubiquitously expressed, and low levels of IRF5 have been reported in murine macrophages.[51,52] Indeed, IRF5 expression in $CD11c^+$ DCs is higher than in BMDMs and $CD11b^+$ (Figures 4H and 4I), suggesting that this transcription factor plays a central role in $CD11c^+$ DCs.

While the data presented in Figures 4A–4G demonstrate that various IRAK1 and IRAK4 regulate IRF5 activation, this effect is likely indirect and may involve the kinase IKKβ.[50,53,54] Accordingly, the IKKβ inhibitors BI605906 and TPCA-1 completely block IRF5 nuclear translocation in $CD11c^+$ DCs stimulated with *T. gondii* and R848 (Figures 4J and S5F) and IL-12 production in splenic $CD11b^+$ and $CD11c^+$ DCs (Figures 4K and S5G–S5I). This is further corroborated by the pattern of p-IKKβ observed in *T. gondii*-exposed $CD11c^+$ DCs (Figures 4L and S5J), which correlates with IRF5 nuclear translocation and IL-12 p40 production, with IRAK1 and IRAK4 greatly impacting IKKβ activation.

These data show that IRF5 drives IL-12 production in $CD11c^+$ DCs and that its activation is controlled by IRAK1 via IKKβ.

IRF5-deficient DCs fail to induce inflammatory molecules

IRF5-deficient $CD11c^+$ DCs failed to produce IL-12 in response to R848 or *T. gondii* Me49, and its activation requires IRAK1 and IRAK4. We next sought to determine whether this transcription factor controls the expression of other inflammatory molecules and how different IRAK mutations impact this production. To achieve this, we quantified the gene transcription 4 h post infection (hpi) with *T. gondii* tachyzoites, using a multiplex inflammatory gene panel (Nanostring) containing probes for 248 genes associated with inflammation in addition to 6 housekeeping controls.

In WT $CD11c^+$ DCs, 66 genes had a log2 fold change above 1 or below −1, along with a —log false discovery rate above 2 (Figure 5A). Next, we prepared a heatmap containing these 66 genes, comparing all of our mutants under uninfected and *T. gondii*-infected conditions. Interestingly, hierarchical analysis revealed a cluster containing all of the uninfected samples in addition to infected *Irak4*$^{-/-}$, *Irak1*$^{-/-}$*Irak2*$^{-/-}$, *Irak1*$^{-/-}$*Irak4* Ki, and *Irf5*$^{-/-}$—evidence that these mutants have severe impairments in the entire inflammatory response to *T. gondii*. The other infected mutants included in our study (*Irak1*$^{-/-}$, *Irak2*$^{-/-}$, *Irak4* Ki, and *Irak2*$^{-/-}$*Irak4* Ki) clustered closer to infected WT DCs, albeit with some modest changes in gene expression (Figure 5B). For instance, our data so far suggest that IRAK1 plays a clear role in IL-12 induction, with IRAK2 being redundant. This pattern is observed not only for *Il12b* but also for *Ccl5*, coding for the chemokine (C-C motif) ligand 5 (CCL5) (Figures S6A and S6B). *Tnf* transcription, however, partially required IRAK1 and IRAK2, as both single KOs showed deficiency (Figure S6C). Induction of all of these molecules required IRF5, as *Irf5*$^{-/-}$ $CD11c^+$ DCs were severely deficient. Not all molecules required IRF5, and the chemokine CCL22 was such an exception; IRF5 deficiency did not decrease *Ccl22* transcription, and only some of the IRAK mutants decreased its transcription (Figure S6D). Validation of these findings by ELISA shows that, at 4 and 24 hpi, the same conclusions can be drawn for IL-12 p40, TNF, and CCL5 (Figures 5C–5F). Interestingly, at 24 hpi, production of CCL22 does

not require IRF5 and only partially requires IRAK4, suggesting that CCL22 induction is only partially myddosome dependent (Figure 5F). Stimulation of TLR7 with R848 revealed similar patterns (Figures S6E–S6H).

CNBP activation by IRAK1 enhances IRF5-mediated IL-12 production in DCs

Our previous study found that CNBP-deficient mice are partially susceptible to *T. gondii* infection and produce lower amounts of IL-12.[8] CNBP nuclear translocation in macrophages is IRAK2 and IRAK4 dependent, and *Cnbp*$^{-/-}$ macrophages are deficient in c-Rel translocation and IL-12 production.[8] This, however, is unlikely to be the mechanism involved in *T. gondii*-exposed DCs, as c-Rel does not induce IL-12 in this context.[33] Based on the findings presented here, we hypothesized that, in *T. gondii*-exposed CD11c^{+} DCs, CNBP activation requires IRAK1, while splenic CD11b^{+} cells require IRAK2. Additionally, since IRF5 drives IL-12 production upon *T. gondii* infection (Figures 4 and 5), we postulated that CNBP is a positive regulator of IRF5 activity.

To investigate these possibilities, we first studied the pattern of CNBP nuclear translocation in *T. gondii*-exposed CD11c^{+} DCs and splenic CD11b^{+} cells. Similar to IRF5 (Figures 4A– 4C), CNBP nuclear translocation in DCs required primarily IRAK1. Similarly, *Irak4* Ki has decreased CNBP translocation, with the residual signal involving the IRAK4 scaffold function in addition to IRAK1, as *Irak1*$^{-/-}$*Irak4* Ki and *Irak4*$^{-/-}$ showed no CNBP translocation (Figures 6A, 6B, S7A, and S7B). In splenic CD11b^{+} cells, CNBP translocation required IRAK2 and the IRAK4 kinase activity (Figures 6C and S7C). As with IRF5 (Figures 4K and 4L), IRAK-mediated CNBP activation requires IKKβ, as this is completely blocked by IKKβ inhibitors (Figure 6D). Importantly, CNBP nuclear translocation occurs independent of IRF5, as *Irf5*$^{-/-}$ behaved like WT DCs (Figures 6A–6E).

To test the links between CNBP and IRF5, we employed CD11c^{+} DCs from *Cnbp*$^{fl/fl}$*Vav-iCre*$^{-/-}$ (control) and *Cnbp*$^{fl/fl}$*Vav-iCre*$^{+/+}$ (CNBP-deficient) mice. These CNBP-deficient CD11c^{+} DCs are partially impaired in IL-12 production in response to R848 and *T. gondii* (Figures 6E and 6F), but IRF5 nuclear translocation is not altered (Figures 6G and S7D). Interestingly, IRF5 and CNBP co-immunoprecipitated upon *T. gondii* stimulation (Figure 6H), suggesting that CNBP might fine-tune IRF5 activity. Indeed, IRF5 binding to the *Il12b* promoter is decreased in CNBP-deficient CD11c^{+} DCs (Figure 6I).

Collectively, these data suggest that (1) CNBP activation requires IRAK2 and IRAK4 kinase activity in splenic CD11b^{+} and IRAK1 in CD11c^{+} DCs, (2) CNBP and IRF5 are independently activated by IKKβ downstream IRAK proteins, and (3) the CNBP and IRF5 interaction enhances IRF5 binding to chromosomal elements near *Il12b*.

IRF5 controls primary infection with *T. gondii*

The finding that IRAK1-dependent activation of IRF5 controls IL-12 production in DCs encouraged us to examine how *Irf5*$^{-/-}$ mice respond to *T. gondii* Me49 infection *in vivo*, as no studies have previously linked this transcription factor to infection with this parasite. As shown in Figure 1, WT C57BL/6 mice immunoprecipitation (IP) infected with *T. gondii* Me49 cysts are resistant to the infection. *Irf5*$^{-/-}$ animals, however, succumb to the infection within 30 days (Figure 7A). This was accompanied by decreased IL-12 p40 in the plasma

and peritoneal cavity as well as decreased IFN-γ in the same compartments (Figures 7B–7E). Accordingly, *Irf5*$^{-/-}$ splenocytes from uninfected animals were also impaired in IL-12 production upon exposure to *T. gondii*, regardless of IFN-γ priming.

These data highlight IRF5 as central in the response against *T. gondii*, controlling the early stages of infection via production of key molecules such as IL-12.

DISCUSSION

Toxoplasmosis is probably the most common human parasite. The Centers for Disease Control and Prevention (CDC) estimate that 11% of the US population above 6 years of age have been infected with *T. gondii*, and some populations in other parts of the world have over 60% of individuals infected. While most individuals are asymptomatic, infection with *T. gondii* is a threat in congenital transmission and immunocompromised hosts. Similarly, congenital infection in sheep and swine is a major cause of stillbirth and abortion, causing major economic losses.[55] As a result of being a natural intermediate host, the rodent innate immune system is adapted to effectively cope with *T. gondii*,[56] and this response is initiated by engagement of endosomal TLRs.[11] Despite its medical and veterinary relevance, many gaps in our understanding of this infection remain. Here, we explored the importance of different IRAK proteins in initiating IL-12 production and host resistance to acute infection with *T. gondii*. We found that, upon activation of endosomal TLRs, IRAK1 is important for the induction of IL-12 by CD11c^{+} DCs, whereas IRAK2 has the dominant role in monocytes and macrophages. Importantly, the release of IL-12 by *T. gondii*-exposed cells requires IRF5 and is fine-tuned by CNBP. Hence, the IRAK/IRF5 axis initiates host resistance to *T. gondii*.

IL-12 initiates IFN-γ production by NK and T cells and mediates host resistance to primary infection with *T. gondii*.[16,17] *In vivo*, the sources of IL-12 during *T. gondii* infection are DCs, MO-DCs, and iMOs,[10,12–15] which recognize PAMPs of the parasite via the endosomal TLR7, TLR9, and TLR11/12.[23,25,26] Engagement of these TLRs leads to IL-12 production via the myddosome, as MyD88 and IRAK4 deficiencies dramatically enhance susceptibility to *T. gondii* infection.[22,31] After recruitment of IRAK4 to the growing myddosome, signaling proceeds with the recruitment of IRAK1 and/or IRAK2.[28] These IRAKs are not completely redundant,[3] and their importance in *T. gondii* infection had not been previously studied. Furthermore, while c-Rel is the transcription factor responsible for IL-12 production in macrophages stimulated with bacterial agonists, this is not the case for *T. gondii* infection.[33] One reason for these gaps in knowledge is the fact that most cell signaling studies focused on macrophages, which are not the main source of IL-12 in *T. gondii*-infected mice.[12] Of note, macrophages are more responsive to LPS, whereas DCs produce higher levels of IL-12 upon activation of TLR7, TLR9, and TLR11/12 by nucleic acids or TgPLP.[25,26,57] Additionally, production of pro-inflammatory cytokines by macrophages requires IRAK2, and the IRAK4 kinase activity is essential.[27,34,37,58] Based on that, we anticipated that *Irak2*$^{-/-}$ would be greatly susceptible to *T. gondii* infection, but surprisingly, *Irak1*$^{-/-}$ and *Irak2*$^{-/-}$ mice had a similar phenotype with small increase in susceptibility. Similarly, we expected *Irak4* Ki to phenocopy *Irak4*$^{-/-}$, which was not the case.

As shown in this study, isolation of splenic CD11c$^+$ DCs and CD11b$^+$ cells (iMOs and MO-DCs) followed by *T. gondii* infection suggests that these cells employ different IRAKs for IL-12 production, with CD11b$^+$ and CD11c$^+$ cells requiring IRAK2 and IRAK1, respectively. This potentially explains why, *in vivo*, IRAK1 and IRAK2 single KO mice only show a subtle phenotype, with increased parasite burden in their brains but not enhanced mortality; in these animals, different cell populations might still produce enough IL-12 to control the infection, and indeed, WT and the single KO mice produce similar levels of IFN-γ upon *T. gondii* infection. Disruption of both IRAK1 and IRAK2, however, dramatically impairs cytokine production in CD11c$^+$ DCs and CD11b$^+$ (iMOs and MO-DCs), and *Irak1*$^{-/-}$*Irak2*$^{-/-}$ mice phenocopy *Irak4*$^{-/-}$ *in vivo*.

It is presently unclear why different cell types employ different IRAKs. The reasons for this are likely multifactorial, but their preference for IRAK1 or IRAK2 correlated with their expression levels, as IRAK2 expression is low in CD11c$^+$ DCs, and IRAK1 expression is low in splenic CD11b$^+$. Thus, signaling relied on the more abundant protein. The observation that different myeloid cells employ different IRAKs in the myddosome raises one intriguing possibility: we speculate that IRAK1 and IRAK2 phosphorylate different targets and that this contributes to the unique phenotypes observed in different cell populations. This hypothesis is substantiated by the fact that IRAK1 is a typical kinase, while IRAK2 has key mutations in its kinase domain and was originally considered a pseudokinase.[59,60] However, IRAK2 does have kinase activity that likely occurs via a non-canonical mechanism.[27,61,62] Furthermore, IRAK1 and IRAK2 have different kinetics upon TLR engagement, with IRAK1 expression decreasing and IRAK2 expression increasing.[5,36,43–45] These factors likely cause different phosphorylation patterns in different populations. Future phosphoproteomics studies may answer these questions.

Although c-Rel is the main transcription factor driving *Il12b* transcription in TLR-stimulated macrophages,[32] c-Rel KO mice infected with *T. gondii* are not impaired in IL-12 production[33] despite showing an impairment in T cells.[63] Indeed, here we observed that the patterns of c-Rel activation in our various IRAK-deficient DCs did not correlate with IL-12 production. IRF5 is also activated by the myddosome of endosomal TLRs, and this transcription factor is known to regulate the expression of pro-inflammatory genes such as TNF, IL-12, and IL-6.[47,49] However, no study has linked *T. gondii* infection to IRF5, which inspired us to study this transcription factor. Here, we observe that, upon *T. gondii* exposure, the patterns of IRF5 activation in our various IRAK-deficient DCs correlated precisely with the patterns of IL-12 production.

IRF5 expression is not ubiquitous.[64] Here, we observed that CD11c$^+$ DCs express high levels of IRF5 compared with BMDMs and splenic CD11b$^+$ cells. Accordingly, IL-12 production is nearly completely blocked in IRF5 KO CD11c$^+$ DCs, and *Irf5*$^{-/-}$ DCs are impaired in the transcription of genes coding for molecules key to controlling the infection, such as *Ccl5* and *Tnf*, in addition to *Il12b*.[16,17,65–67] IRF5 activation could also explain why IRAK1 has a more prevalent role in DCs, as previous work done in HEK cells has suggested that IRAK1, and not IRAK2, is responsible for IRF5 activation.[68–70] We observe that, at endogenous protein levels in murine DCs, IRAK1 is indeed responsible for IRF5 activation, as *Irak1*$^{-/-}$ CD11c$^+$ DCs show greatly reduced IRF5 nuclear translocation upon

exposure to *T. gondii*. IRF5 activation in CD11c$^+$ DCs also requires the IRAK4 scaffold, but surprisingly, loss of IRAK4 kinase activity only partially inhibits IRF5 activation. This residual activation is mediated by IRAK1, as no IRF5 translocation is observed in *Irak1*$^{-/-}$*Irak4* Ki DCs. However, our study suggests that IRAK2 can lead to IRF5 activation, as the small IRF5 nuclear translocation observed in *Irak1*$^{-/-}$ CD11c$^+$ DCs is completely absent in *Irak1*$^{-/-}$*Irak2*$^{-/-}$ and IRF5 nuclear translocation in CD11b$^+$ cells. This IRAK-dependent IRF5 activation is likely indirect and involves IKKβ.[53,54] Activation of IRF5 also involves the endosomal transporter SLC15A4, which recruits the protein TasL and mediates IRF5 recruitment to the endosome.[50,71] It is presently unclear whether IRAKs are required for the activities of SLC15A4 or TasL.

The discovery that IRF5 is the main transcription factor responsible for IL-12 production in *T. gondii*-infected CD11c$^+$ DCs led us to reevaluate the role of CNBP. In LPS-stimulated macrophages, IRAK4 and IRAK2 activity leads to CNBP activation, which controls IL-12 expression by regulating c-Rel nuclear translocation.[8] CNBP KO animals are partially susceptible to *T. gondii* infection, with decreased IL-12 production *in vivo*.[8] This could not be mediated by c-Rel, as this protein is not involved in IL-12 produced in response to *T. gondii*;[33] thus, we hypothesized that CNBP regulates IRF5 activity. Indeed, we found that CNBP modulates IRF5 binding to DNA, as CNBP-deficient CD11c$^+$ DCs showed normal IRF5 nuclear translocation but lower IRF5 binding to the *Il12b* promoter. We also demonstrated that, upon *T. gondii* exposure, IRF5 and CNBP physically interact, although it is unclear whether this is a direct interaction or whether they are part of a larger DNA-bound complex. Similar results have been described linking IRF3 and IRF7 to CNBP, with evidence of physical interaction, modulation of their affinity to promoter regions, and no impact on nuclear translocation.[72] Importantly, the pattern of CNBP nuclear translocation differs between CD11c$^+$ DCs and CD11b$^+$ (iMOs and MO-DCs), with IRAK1 playing an essential role in DCs, while iMOs, MO-DCs and BMDMs employ IRAK2.[8] Although the molecular mechanism linking CNBP to these IRFs remains poorly understood, the idea that CNBP regulates the activity of many transcription factors is an exciting perspective.

T. gondii-infected *Irf5*$^{-/-}$ cells showed a dramatic reduction in IL-12 output. This suggested that IRF5-deficient animals would be highly susceptible to *T. gondii* infection. Indeed, IP infection with *T. gondii* Me49 cysts revealed enhanced mortality in IRF5 KO mice in comparison with the WT, with animals succumbing within 30 days of infection. This was accompanied by low levels of IL-12 and IFN-γ, especially in the peritoneal cavity, a decreased that is also observed in highly susceptible mouse strains such as *Irak1*$^{-/-}$*Irak2*$^{-/-}$ and *Irak4*$^{-/-}$ and mice carrying missense UNC93B1.[23,24,26,31] Responses triggered by endosomal TLRs are of paramount importance in protection against parasites such as *Trypanosoma cruzi*, *Trypanosoma brucei*, and *Leishmania major*.[73–75] Therefore, we speculate that IRF5 also plays an important role in controlling these infections.

In summary our findings demonstrate that, in murine DCs, the IRAK1/IRF5 axis drives the production of key inflammatory molecules such as IL-12, CCL5, and TNF. The IRF5 activity is further modulated by CNBP, which is independently activated by the myddosome. This highlights that IRF5 is central in controlling parasitic infections via production of IL-12.

Limitations of the study

The data presented in this article were obtained using mouse infection models. Generalizations to other species should be done carefully, as the repertoire of TLRs expressed may differ from organism to organism.[2] We acknowledge that *Irf5*$^{-/-}$ animals, while susceptible to *T. gondii* infection, are not completely impaired in IL-12 production. Therefore, we cannot rule out that other transcription factors may play a role in the *in vivo* response.

STAR★METHODS

RESOURCE AVAILABILITY

Lead contact—Further information and resource requests can be directed to and will be fulfilled by the lead contact Ricardo T. Gazzinelli (ricardo.gazzinelli@umassmed.edu).

Materials availability—Mouse lines and cell lines used in this study are available from the lead contact with a completed Materials Transfer Agreement.

Data and code availability

- The uncropped immunoblots and quantitative data have been deposited at Mendeley Data and are publicly available as of the date of publication. DOIs are listed in the key resource table.
- This paper does not report original code.
- Any additional information required to reanalyse the data reported in this work paper is available from the lead contact upon request.

EXPERIMENTAL MODEL AND STUDY PARTICIPANT DETAILS

Mice—C57BL/6 WT, *Irak1*$^{-/-}$,[35] *Irak2*$^{-/-}$[58] and *Vav-iCre*[76] mice were acquired from The Jackson Laboratory. *Irak4*$^{-/-}$ was provided by Dr. Tak Mak (Princess Margaret Cancer Center, University of Toronto, Toronto, Canada).[29] *Irak4* Ki mice were provided by Dr. Xiaoxia Li (Department of Inflammation and Immunity, Lerner Research Institute, Cleveland Clinic, Cleveland, USA).[37] *Irf5*$^{-/-}$ was provided by Dr. Betsy J. Barnes (Institute of Molecular Medicine, Feinstein Institutes for Medical Research, New York, USA).[47] *Cnbp*$^{fl/fl}$ was generated as described previously and crossed in house with *Vav-iCre*.[72] *Irak1*$^{-/-}$*Irak2*$^{-/-}$, *Irak1*$^{-/-}$*Irak4* Ki and *Irak2*$^{-/-}$*Irak4* Ki were generated by in-house crossing.

All animal procedures were performed in accordance with the guidelines of the National Institutes of Health and were approved by the Institutional Animal Care and Use Committee (IACUC) at the University of Massachusetts Chan Medical School (protocol 202100193). This work used male and female mice in similar proportions, with ages ranging from 8 to 12 weeks old.

METHOD DETAILS

Chemicals—The following chemicals were routinely used in this project: Ethanol (molecular biology grade) (Fisher Scientific), NaF (Sigma-Aldrich), $NaVO_4$ (Sigma-Aldrich), b-Glycerophosphate disodium (Santa Cruz), Nonidet P-40 Substitute (NP-40) (Boston Bioproducts), Dulbecco's Modified Eagle Medium (DMEM) (Corning), Dulbecco's Phosphate Buffered Saline (PBS) (Corning), Tris-Buffered Saline (TBS) (Boston Bioproducts) and Tween 20 (Boston Bioproducts).

In vivo* T. gondii infections—T. gondii* Me49 strain was maintained *in vivo* in WT C57BL/6 mice by intraperitoneal inoculation of brain homogenates containing *T. gondii* Me49 cysts every 45 days (5 cysts per mouse). *In vivo* infection assays were performed by intraperitoneal inoculation of *T. gondii* Me49 (25 cysts per mouse), or mock-infected with PBS (uninfected control). Mice survival was followed up to 40 days post-infection. The surviving animals were sacrificed by CO_2 exposure followed by cervical dislocation in accordance with UMMS IACUC guidelines, and the number of cysts in the brain was counted by optical microscopy.

Cell isolation and culture—For isolation of bone marrow and generation of BMDMs, mice were sacrificed by CO_2 exposure followed by cervical dislocation in accordance with UMMS IACUC guidelines, the skin was then sterilized with 70% isopropanol, the legs removed, the tibia and femur were collected, the bone marrow was flushed out of the bone using BMDM complete media (DMEM supplemented with 10% fetal bovine serum (R&D Systems), 5 mM L-Glutamine (GIBCO), 25 mM HEPES (Thermo-Fisher) and 20% L929-conditioned media). The bone marrow cells of each animal were then placed in 3 untreated 150 mm × 15 mm petri dishes (Corning) and kept at 37°C and 5% CO_2 in BMDM complete media for 6 to 9 days. For splenocyte isolation, mice were sacrificed as described above, the spleen collected, macerated in a 100 mm nylon cell strainer, and the red blood cells lysed in ACK Lysing Buffer (Gibco) for 5 min at room temperature. The splenocytes were then washed twice and resuspended in DMEM containing 10% FBS. For isolation of $CD11b^+$ cells, splenocytes were incubated for 24 h at 37°C and 5% CO_2 with 100 ng mL^{-1} IFN-γ (BioLegend), and positive selection using CD11b microbeads (Miltenyi) performed according to the manufacturer's instructions. Isolation of $CD11c^+$ DCs was performed by subcutaneous inoculation of 10^6 B16-$Flt3l^+$ cells,[77] and after 12 to 15 days, the animals were sacrificed as described above, the spleen collected, the splenocytes prepared as described above, and $CD11c^+$ cells were isolated by positive selection using CD11c microbeads (Miltenyi) according to the manufacturer's instructions.

T. gondii Me49 tachyzoites were maintained *in vitro* by weekly infections in human foreskin fibroblasts in DMEM containing 10% FBS and cultured at 37°C and 5% CO_2.[78] IKKβ inhibition experiments included a pre-incubation step of 30 min at 37°C and 5% CO_2 with BI605906 10 μM (Millipore-Sigma) or TPCA-1 10 μM (Cell Signaling).

Flow cytometry—To determine the population of monocytes (MO), iMOs and MO-DCs, splenocytes were isolated and treated with IFN-γ (100 ng mL^{-1}, 24 h) (BioLegend) or left unstimulated. After treatment, cells were washed three times (400 x G, 5 min, 4°C)

in ice-cold FACS Buffer (PBS containing 0.5% FBS and 2 mM EDTA) and transferred to a 96-wells U-bottom plate (Corning) (10^6 cells/well). The cells were stained with Live/Dead Ghost Aqua V510 (1:250, Tonbo Biosciences) to exclude death cells, then blocked with mouse CD16/32 (clone 93, 1:100, BioLegend) for 20 min at 4°C. After one wash in FACS Buffer, cells were stained for 30 min at 4°C with the following antibodies: F4/80 (clone BM8) PE-Cy5 (1:100, BioLegend), CD11b (clone M1/70) PE-Cy7 (1:4000, BioLegend), DCSign (clone MMD3) eFluor660 (1:800, Thermo Fisher), and MHCII (clone AF6–120.1) PE (1:400, BioLegend). Cells were washed twice, and sample acquisition was immediately performed on a Cytek Aurora Spectral Cytometer. *Fluorescence minus one* (FMO) samples were included to ensure accurate selection of positive populations. Data analysis was performed on FlowJo v10 (BD).

Preparation of whole cell lysates and nuclear extracts—For preparation of whole cell lysates, treated or untreated cells were washed three times in ice-cold PBS containing 25 mM β-Glycerophosphate disodium, 10 mM NaF and 1 mM $NaVO_4$, and lysed for 10 min on ice with Tris-HCl 50 mM, NaCl 150 mM, EDTA 5 mM, 1% NP-40, Halt Protease inhibitor (Thermo-Fisher) and Halt Phosphatase inhibitor (Thermo-Fisher). In selected experiments, whole cell lysates were prepared by treating the cells for 10 min on ice with Tris-HCl 50 mM, NaCl 150 mM, 1% NP-40 and 1 mM phenyl-methanesulfonyl fluoride (Sigma-Aldrich), followed by 60 min incubation in HEPES 50 mM pH 7.5, 2 mM DTT, 0.01% Brij-35, MnCl2 1 mM, λ phosphatase (2 U μL^{-1}) and ubiquitin specific peptidase 2 (USP) 1 μM.

For preparation of nuclear extracts, treated or untreated cells were subjected to cell lysis and nuclear fractionation using NE-Per Nuclear and Cytoplasmic Extraction Reagents (Thermo-Fisher) as described by the manufacturer.

Co-immunoprecipitation—In 5 mL conical tubes, 4×10^6 cells were left unstimulated or exposed to *T. gondii* Me49 tachyzoites (MOI 3), washed three times in cold PBS containing 25 mM β-Glycerophosphate disodium, 10 mM NaF and 1 mM $NaVO_4$, and lysed for 10 min on ice with 0.5 mL of IP lysis buffer (50 mM Tris-HCl pH 7.5, 150 mM NaCl, 1 mM EDTA, 1% NP-40, 10% glycerol, 10 mM iodoacetamide, Halt Protease inhibitor (Thermo-Fisher) and Halt Phosphatase inhibitor (Thermo-Fisher)). The lysates were then centrifuged at 12000 x G for 10 min at 4°C, and the supernatants collected. 50 μL of the supernatant was kept for analysis of the protein input, while the remainder was used for co-immunoprecipitation. 5 μL of anti-IRF5 (Cell Signaling, 4950) and 30 μL of Protein G Sepharose 4 Fast Flow (Millipore Sigma) pre-equilibrated with IP lysis buffer was added to each sample. The samples were then incubated with gentle agitation for 16 h at 4°C, washed three times with IP lysis buffer, eluted with 50 μL of 1x sample buffer (Pierce Lane Reducing Sample Buffer (Thermo-Fisher)), and immunoblots were then carried out as described below.

Immunoblot—Protein extracts were incubated with Pierce Lane Reducing Sample Buffer (Thermo-Fisher) at 100°C for 10 min, loaded on polyacrylamide gels and electrophoresis was performed. The proteins were transferred to 0.45 μm nitrocellulose membrane (Amersham Protran 0.45 NC, Millipore Sigma) or polyvinylidene fluoride (Immobilon-P

PVDF 0.45, Millipore Sigma) in wet transfer buffer (25 mM tris-base, 192 mM glycine, 20% methanol, pH 8.5) for 20 h at 50 mA. The membranes were blocked for 2 h at room temperature in 5% blotting-grade blocker (Bio-Rad), incubated with primary antibody in TBS containing BSA 1% for 16 h at 4°C, washed with TBS containing 0.1% Tween 20 (TBS-T) (three times, 5 min each), incubated with secondary antibody in 5% blotting-grade blocker for 1 h and washed three times in TBS-T. Proteins were detected using Clarity Max ECL Substrate (Bio-Rad) and imaged in ChemiDoc MP Imaging System (Bio-Rad). Densitometric analysis were performed using ImageJ (NIH).[79]

The following antibodies and dilutions were used: IRAK1 (Cell Signaling, 4504S, 1:1000), IRAK2 (Abcam, ab62419, 1:500), IRAK4 (Novus, NB500–597, 1:1000), MyD88 (R&D Systems, AF3109, 1:500), rodent-specific IRF5 (Cell Signaling, 4950, 1:1000), USF2 (Novus Biologicals, NBP1–92649, 1:2000), c-Rel (Cell Signaling, 67489, 1:1000), phospho-IκB-α (Ser32) (Cell Signaling, 2859, 1:750), IκB-α (Cell Signaling, 4812S, 1:1000), phospho-RelA/NF-κB (Ser 536) (Cell Signaling, 3033, 1:1000), RelA/NF-κB (Novus Biologicals, NB100–2176, 1:1000), Actin (Sigma-Aldrich, A2066, 1:3000), phospho-SAPK/JNK (Thr 183/Tyr 185) (Cell Signaling, 4668T, 1:1000), phospho-p38 MAPK (Thr 180/Tyr 182) (Cell Signaling, 4511T, 1:1000), phospho-p44/42 MAPK (Erk 1/2) (Thr 202/Tyr 204) (Cell Signaling, 4370T, 1:2000), phosphor-IKK (Ser 176/180) (Cell Signaling, 2697, 1:1000), CNBP (Santa Cruz, sc-515387-X, 1:200), anti-Goat-IgG HRP-conjugated (R&D Systems, HAF017, 1:5000), anti-Rabbit-IgG HRP-conjugated (Sigma-Aldrich, A0545, 1:5000), anti-Mouse-IgG HRP-conjugated (Cell Signaling, 7076S, 1:5000).

Transcription analysis—CD11c+ DCs were isolated as described above, and two identical 24-well plates were prepared containing 1×10^6 cells per well. Cells were then left untreated, treated with 1 μg mL^{-1} R848 (Invivogen) or infected with *T. gondii* Me49 tachyzoites (MOI 3), in a final volume of 500 μL per well, and incubated for 4 or 24 h (37°C and 5% CO_2). The 24-h plate had their supernatants collected for cytokine/chemokine quantification. The 4-h plate had their supernatants collected for cytokine/chemokine quantification, while the cells were collected from each well, washed three times in cold PBS containing 25 mM β-Glycerophosphate disodium, 10 mM NaF and 1 mM $NaVO_4$, and their RNA extracted using RNeasy micro kit (QIAGEN) as described by the manufacturer. For each sample, 40 ng of RNA was hybridized for 16 h at 65°C with capture and reporter probes (Mm_V2_Inflammation_CSO, 115000082, NanoString). The hybridized samples were loaded onto the nCounter station. Analysis was performed using the nSolver software version 4.0 for Mac (NanoString). Hierarchical clustering was performed using Morpheus (https://software.broadinstitute.org/morpheus).

ChIP assays—CD11c+ DCs were isolated as described above, and 5×10^6 cells were incubated with media alone or *T. gondii* Me49 tachyzoites (MOI 3) for 2 h (37°C and 5% CO_2) in 5 mL conical tubes in a final volume of 2 mL. After treatments, cells were washed three times in ice-cold PBS containing 25 mM β-Glycerophosphate disodium, 10 mM NaF and 1 mM $NaVO_4$. The cells were then fixed in 1% formaldehyde (Thermo-Fisher), the nuclear fraction isolated and ChIP was performed as described by the manufacturer (Pierce Agarose ChIP kit, Thermo-Fisher) using 2 μL of normal rabbit IgG (2729S, Cell Signaling)

or 5 μL of anti-IRF5 rodent specific (4950, Cell Signaling). The *Il12b* promoter region containing the interferon-stimulated response element (ISRE) was then quantified in relation to input by quantitative PCR using the primers: 5°-ACCCCGAAGTCATTTCCTCT-3′ and 5′-ACCCACTGTTCCTTCTGCT-3′.[47]

Cytokine quantifications—For cell stimulations, 100.000 cells were plated in flat-bottom 96-well plates (Corning) and immediately stimulated with 1 μg mL^{-1} R848 (Invivogen) or *T. gondii* Me49 at MOI 3 for up to 24 h (37°C and 5% CO_2). The culture supernatants were then collected. Cytokine and chemokine quantification was performed from culture supernatants, peritoneal lavage or serum, according to the manufacturer instructions: IL-12 p40 Mouse uncoated ELISA kit (Invitrogen, 88–7120-88), Mouse CCL5/Rantes DuoSet ELISA (R&D Systems, DY478), Mouse TNF-alpha DuoSet ELISA (R&D Systems, DY410), Mouse Interferon-gamma DuoSet ELISA (R&D Systems, DY485), and Mouse CCL22 DuoSet ELISA (R&D Systems, DY439).

QUANTIFICATION AND STATISTICAL ANALYSIS

Statistical analysis was performed using GraphPad Prism 9.5 for macOS (GraphPad Software). Experiments in this work employed one-way analysis of variance (ANOVA) with Tukey post-comparison test for comparisons between multiple groups: *p < 0.05, **p < 0.01, ***p < 0.001. ****p < 0.0001. Unpaired t test was used in experiments comparing only two groups: #p < 0.05, ##p < 0.01, ###p < 0.001. ####p < 0.0001. Error bars represent standard error of the mean (SEM). Comparisons between survival curves was performed using the log rank (Mantel-Cox) test. Statistical details of experiments can be found in the figure legends.

Supplementary Material

Refer to Web version on PubMed Central for supplementary material.

ACKNOWLEDGMENTS

We are grateful to Dr. Betsy J. Barnes, Dr. Jonathan Pruneda, Dr. Stephen Smale, Larissa Pereira, and Dr. Romana Rashid. This work was partially supported by the National Institutes of Health (R01NS098747, R01AI079293, R01AI060025, and 2U19 AI089681) and the Brazilian National Institute of Science and Technology for Vaccines granted by Conselho Nacional de Desenvolvimento Científico e Tecnoló gico (CNPq)/Fundaçaõ de Amparo à Pesquisa do Estado de Minas Gerais (Fapemig)/Coordenaç aõ de Aperfeiç oamento de Pessoal de Ensino Superior (CAPES) (465293/2014–0).

REFERENCES

1. Akira S, Uematsu S, and Takeuchi O, (2006). Pathogen Recognition and Innate Immunity. Cell 124, 783–801. 10.1016/j.cell.2006.02.015. [PubMed: 16497588]
2. Fitzgerald KA, and Kagan JC (2020). Toll-like Receptors and the Control of Immunity. Cell 180, 1044–1066. 10.1016/j.cell.2020.02.041. [PubMed: 32164908]
3. Pereira M, and Gazzinelli RT (2023). Regulation of innate immune signaling by IRAK proteins. Front. Immunol. 14, 1133354.
4. Cao Z, Xiong J, Takeuchi M, Kurama T, and Goeddel DV (1996). TRAF6 is a signal transducer for interleukin-1. Nature 383, 443–446. 10.1038/383443a0. [PubMed: 8837778]

5. Pauls E, Nanda SK, Smith H, Toth R, Arthur JSC, and Cohen P (2013). Two Phases of Inflammatory Mediator Production Defined by the Study of IRAK2 and IRAK1 Knock-in Mice. J.I. 191, 2717–2730. 10.4049/jimmunol.1203268.
6. Silverman N, and Maniatis T (2001). NF-κB signaling pathways in mammalian and insect innate immunity. Genes Dev. 15, 2321–2342. 10.1101/gad.909001. [PubMed: 11562344]
7. Lee E, Lee TA, Kim JH, Park A, Ra EA, Kang S, Choi HJ, Choi JL, Huh HD, Lee JE, et al. (2017). CNBP acts as a key transcriptional regulator of sustained expression of interleukin-6. Nucleic Acids Res. 45, 3280–3296. 10.1093/nar/gkx071. [PubMed: 28168305]
8. Chen Y, Sharma S, Assis PA, Jiang Z, Elling R, Olive AJ, Hang S, Bernier J, Huh JR, Sassetti CM, et al. (2018). CNBP controls IL-12 gene transcription and Th1 immunity. J. Exp. Med. 215, 3136–3150. 10.1084/jem.20181031. [PubMed: 30442645]
9. Elmore SA, Jones JL, Conrad PA, Patton S, Lindsay DS, and Dubey JP (2010). Toxoplasma gondii: epidemiology, feline clinical aspects, and prevention. Trends Parasitol. 26, 190–196. 10.1016/j.pt.2010.01.009. [PubMed: 20202907]
10. Gazzinelli RT, Mendonc¸a-Neto R, Lilue J, Howard J, and Sher A (2014). Innate resistance against Toxoplasma gondii: An evolutionary tale of mice, cats, and men. Cell Host Microbe 15, 132–138. 10.1016/j.chom.2014.01.004. [PubMed: 24528860]
11. Yarovinsky F (2014). Innate immunity to Toxoplasma gondii infection. Nat. Rev. Immunol. 14, 109–121. 10.1038/nri3598. [PubMed: 24457485]
12. Reis e Sousa C, Hieny S, Scharton-Kersten T, Jankovic D, Charest H, Germain RN, and Sher A (1997). In Vivo Microbial Stimulation Induces Rapid CD40 Ligand–independent Production of Interleukin 12 by Dendritic Cells and their Redistribution to T Cell Areas. J. Exp. Med. 186, 1819–1829. 10.1084/jem.186.11.1819. [PubMed: 9382881]
13. Dunay IR, DaMatta RA, Fux B, Presti R, Greco S, Colonna M, and Sibley LD (2008). Gr1+ Inflammatory Monocytes Are Required for Mucosal Resistance to the Pathogen Toxoplasma gondii. Immunity 29, 306–317. 10.1016/j.immuni.2008.05.019. [PubMed: 18691912]
14. Goldszmid RS, Caspar P, Rivollier A, White S, Dzutsev A, Hieny S, Kelsall B, Trinchieri G, and Sher A (2012). NK Cell-Derived Interferon-g Orchestrates Cellular Dynamics and the Differentiation of Monocytes into Dendritic Cells at the Site of Infection. Immunity 36, 1047–1059. 10.1016/j.immuni.2012.03.026. [PubMed: 22749354]
15. Mashayekhi M, Sandau MM, Dunay IR, Frickel EM, Khan A, Goldszmid RS, Sher A, Ploegh HL, Murphy TL, Sibley LD, and Murphy KM (2011). CD8a+ Dendritic Cells Are the Critical Source of Interleukin-12 that Controls Acute Infection by Toxoplasma gondii Tachyzoites. Immunity 35, 249–259. 10.1016/j.immuni.2011.08.008. [PubMed: 21867928]
16. Gazzinelli RT, Hieny S, Wynn TA, Wolf S, and Sher A (1993). Interleukin 12 is required for the T-lymphocyte-independent induction of interferon gamma by an intracellular parasite and induces resistance in T-cell-deficient hosts. Proc. Natl. Acad. Sci. USA 90, 6115–6119. 10.1073/pnas.90.13.6115. [PubMed: 8100999]
17. Gazzinelli RT, Wysocka M, Hayashi S, Denkers EY, Hieny S, Caspar P, Trinchieri G, and Sher A (1994). Parasite-induced IL-12 stimulates early IFN-gamma synthesis and resistance during acute infection with Toxoplasma gondii. J. Immunol. 153, 2533–2543. 10.4049/jimmunol.153.6.2533. [PubMed: 7915739]
18. Tabeta K, Hoebe K, Janssen EM, Du X, Georgel P, Crozat K, Mudd S, Mann N, Sovath S, Goode J, et al. (2006). The Unc93b1 mutation 3d disrupts exogenous antigen presentation and signaling via Toll-like receptors 3, 7 and 9. Nat. Immunol. 7, 156–164. 10.1038/ni1297. [PubMed: 16415873]
19. Kim Y-M, Brinkmann MM, Paquet M-E, and Ploegh HL (2008). UNC93B1 delivers nucleotide-sensing toll-like receptors to endolysosomes. Nature 452, 234–238. 10.1038/nature06726. [PubMed: 18305481]
20. Lee BL, Moon JE, Shu JH, Yuan L, Newman ZR, Schekman R, and Barton GM (2013). UNC93B1 mediates differential trafficking of endosomal TLRs. Elife 2, e00291. 10.7554/eLife.00291.
21. Majer O, Liu B, Woo BJ, Kreuk LSM, Van Dis E, and Barton GM (2019). Release from UNC93B1 reinforces the compartmentalized activation of select TLRs. Nature 575, 371–374. 10.1038/s41586-019-1611-7. [PubMed: 31546247]

22. Scanga CA, Aliberti J, Jankovic D, Tilloy F, Bennouna S, Denkers EY, Medzhitov R, and Sher A (2002). Cutting Edge: MyD88 Is Required for Resistance to Toxoplasma gondii Infection and Regulates Parasite-Induced IL-12 Production by Dendritic Cells. J. Immunol. 168, 5997–6001. 10.4049/jimmunol.168.12.5997. [PubMed: 12055206]
23. Melo MB, Kasperkovitz P, Cerny A, Kö nen-Waisman S, Kurt-Jones EA, Lien E, Beutler B, Howard JC, Golenbock DT, and Gazzinelli RT (2010). UNC93B1 Mediates Host Resistance to Infection with Toxoplasma gondii. PLoS Pathog. 6, e1001071. 10.1371/journal.ppat.1001071.
24. Pifer R, Benson A, Sturge CR, and Yarovinsky F (2011). UNC93B1 Is Essential for TLR11 Activation and IL-12-dependent Host Resistance to Toxoplasma gondii. J. Biol. Chem. 286, 3307–3314. 10.1074/jbc.M110.171025. [PubMed: 21097503]
25. Yarovinsky F, Zhang D, Andersen JF, Bannenberg GL, Serhan CN, Hayden MS, Hieny S, Sutterwala FS, Flavell RA, Ghosh S, and Sher A (2005). TLR11 Activation of Dendritic Cells by a Protozoan Profilin-Like Protein. Science 308, 1626–1629. 10.1126/science.1109893. [PubMed: 15860593]
26. Andrade WA, Souza M.d.C., Ramos-Martinez E, Nagpal K, Dutra MS, Melo MB, Bartholomeu DC, Ghosh S, Golenbock DT, and Gazzinelli RT (2013). Combined Action of Nucleic Acid-Sensing Toll-like Receptors and TLR11/TLR12 Heterodimers Imparts Resistance to Toxoplasma gondii in Mice. Cell Host Microbe 13, 42–53. 10.1016/j.chom.2012.12.003. [PubMed: 23290966]
27. Kawagoe T, Sato S, Matsushita K, Kato H, Matsui K, Kumagai Y, Saitoh T, Kawai T, Takeuchi O, and Akira S (2008). Sequential control of Toll-like receptor-dependent responses by IRAK1 and IRAK2. Nat. Immunol. 9, 684–691. 10.1038/ni.1606. [PubMed: 18438411]
28. Lin SC, Lo YC, and Wu H (2010). Helical assembly in the MyD88-IRAK4-IRAK2 complex in TLR/IL-1R signalling. Nature 465, 885–890. 10.1038/nature09121. [PubMed: 20485341]
29. Suzuki N, Suzuki S, Duncan GS, Millar DG, Wada T, Mirtsos C, Takada H, Wakeham A, Itie A, Li S, et al. (2002). Severe impairment of interleukin-1 and toll-like receptor signalling in mice lacking IRAK-4. Nature 416, 750–756. 10.1038/nature736. [PubMed: 11923871]
30. von Bernuth H, Picard C, Puel A, and Casanova J-L (2012). Experimental and natural infections in MyD88-and IRAK-4-deficient mice and humans. Eur. J. Immunol. 42, 3126–3135. 10.1002/eji.201242683. [PubMed: 23255009]
31. Bé la SR, Dutra MS, Mui E, Montpetit A, Oliveira FS, Oliveira SC, Arantes RME, Antonelli LR, Mcleod R, and Gazzinelli RT (2012). Impaired innate immunity in mice deficient in interleukin-1 receptor-associated kinase 4 leads to defective type 1 t cell responses, b cell expansion, and enhanced susceptibility to infection with toxoplasma gondii. Infect. Immun. 80, 4298–4308. 10.1128/IAI.00328-12. [PubMed: 23027530]
32. Sanjabi S, Hoffmann A, Liou HC, Baltimore D, and Smale ST (2000). Selective requirement for c-Rel during IL-12 P40 gene induction macrophages. Proc. Natl. Acad. Sci. USA 97, 12705–12710. 10.1073/pnas.230436397. [PubMed: 11058167]
33. Mason N, Aliberti J, Caamano JC, Liou H-C, and Hunter CA (2002). Cutting Edge: Identification of c-Rel-Dependent and -Independent Pathways of IL-12 Production During Infectious and Inflammatory Stimuli. J. Immunol. 168, 2590–2594. 10.4049/jimmunol.168.6.2590. [PubMed: 11884420]
34. Pereira M, Durso DF, Bryant CE, Kurt-Jones EA, Silverman N, Golenbock DT, and Gazzinelli RT (2022). The IRAK4 scaffold integrates TLR4-driven TRIF and MYD88 signaling pathways. Cell Rep. 40, 111225. 10.1016/j.celrep.2022.111225.
35. Thomas JA, Allen JL, Tsen M, Dubnicoff T, Danao J, Liao XC, Cao Z, and Wasserman SA (1999). Impaired Cytokine Signaling in Mice Lacking the IL-1 Receptor-Associated Kinase. J. Immunol. 163, 978–984. [PubMed: 10395695]
36. De Nardo D, Balka KR, Cardona Gloria Y, Rao VR, Latz E, and Masters SL (2018). Interleukin-1 receptor-associated kinase 4 (IRAK4) plays a dual role in myddosome formation and Toll-like receptor signaling. J. Biol. Chem. 293, 15195–15207. 10.1074/jbc.RA118.003314. [PubMed: 30076215]
37. Kim TW, Staschke K, Bulek K, Yao J, Peters K, Oh KH, Vanden-burg Y, Xiao H, Qian W, Hamilton T, et al. (2007). A critical role for IRAK4 kinase activity in Toll-like receptor-mediated innate immunity. J. Exp. Med. 204, 1025–1036. 10.1084/jem.20061825. [PubMed: 17470642]

38. Snyder LM, Doherty CM, Mercer HL, and Denkers EY (2021). Induction of IL-12p40 and type 1 immunity by Toxoplasma gondii in the absence of the TLR-MyD88 signaling cascade. PLoS Pathog. 17, e1009970. 10.1371/journal.ppat.1009970.
39. Sukhumavasi W, Egan CE, Warren AL, Taylor GA, Fox BA, Bzik DJ, and Denkers EY (2008). TLR Adaptor MyD88 Is Essential for Pathogen Control during Oral Toxoplasma gondii Infection but Not Adaptive Immunity Induced by a Vaccine Strain of the Parasite. J. Immunol. 181, 3464–3473. 10.4049/jimmunol.181.5.3464. [PubMed: 18714019]
40. Kawagoe T, Sato S, Jung A, Yamamoto M, Matsui K, Kato H, Uematsu S, Takeuchi O, and Akira S (2007). Essential role of IRAK-4 protein and its kinase activity in Toll-like receptor-mediated immune responses but not in TCR signaling. J. Exp. Med. 204, 1013–1024. 10.1084/jem.20061523. [PubMed: 17485511]
41. Pennini ME, Perkins DJ, Salazar AM, Lipsky M, and Vogel SN (2013). Complete Dependence on IRAK4 Kinase Activity in TLR2, but Not TLR4, Signaling Pathways Underlies Decreased Cytokine Production and Increased Susceptibility to Streptococcus pneumoniae Infection in IRAK4 Kinase–Inactive Mice. J. Immunol. 190, 307–316. 10.4049/jimmunol.1201644. [PubMed: 23209321]
42. Assis PA, Fernandes Durso D, Chacon Cavalcante F, Zaniratto R, Carvalho-Silva AC, Cunha-Neto E, Golenbock DT, Rodrigues Pinto Ferreira L, and Tostes Gazzinelli R (2020). Integrative analysis of micro-RNA and mRNA expression profiles of monocyte-derived dendritic cells differentiation during experimental cerebral malaria. J. Leukoc. Biol. 108, 1183–1197. 10.1002/JLB.1MA0320-731R. [PubMed: 32362022]
43. Yamin T-T, and Miller DK (1997). The Interleukin-1 Receptor-associated Kinase Is Degraded by Proteasomes following Its Phosphorylation. J. Biol. Chem. 272, 21540–21547. 10.1074/jbc.272.34.21540. [PubMed: 9261174]
44. Kubo-Murai M, Hazeki K, Nigorikawa K, Omoto T, Inoue N, and Hazeki O (2008). IRAK-4-dependent Degradation of IRAK-1 is a Negative Feedback Signal for TLR-mediated NF-κB Activation. J. Biochem. 143, 295–302. 10.1093/jb/mvm234. [PubMed: 18079163]
45. Petrova T, Zhang J, Nanda SK, Figueras-Vadillo C, and Cohen P (2021). HOIL-1-catalysed, ester-linked ubiquitylation restricts IL-18 signaling in cytotoxic T cells but promotes TLR signalling in macrophages. FEBS J. 288, 5909–5924. 10.1111/febs.15896. [PubMed: 33932090]
46. Hayden MS, and Ghosh S (2008). Shared Principles in NF-κB Signaling. Cell 132, 344–362. 10.1016/j.cell.2008.01.020. [PubMed: 18267068]
47. Takaoka A, Yanai H, Kondo S, Duncan G, Negishi H, Mizutani T, Kano SI, Honda K, Ohba Y, Mak TW, and Taniguchi T (2005). Integral role of IRF-5 in the gene induction programme activated by Toll-like receptors. Nature 434, 243–249. 10.1038/nature03308. [PubMed: 15665823]
48. Paun A, Reinert JT, Jiang Z, Medin C, Balkhi MY, Fitzgerald KA, and Pitha PM (2008). Functional Characterization of Murine Interferon Regulatory Factor 5 (IRF-5) and Its Role in the Innate Antiviral Response. J. Biol. Chem. 283, 14295–14308. 10.1074/jbc.M800501200. [PubMed: 18332133]
49. Chow KT, Wilkins C, Narita M, Green R, Knoll M, Loo Y-M, and Gale M (2018). Differential and overlapping immune programs regulated by IRF3 and IRF5 in plasmacytoid dendritic cells. J. Immunol. 201, 3036–3050. 10.4049/jimmunol.1800221. [PubMed: 30297339]
50. Heinz LX, Lee J, Kapoor U, Kartnig F, Sedlyarov V, Papakostas K, Cé sar-Razquin A, Essletzbichler P, Goldmann U, Stefanovic A, et al. (2020). TASL is the SLC15A4-associated adaptor for IRF5 activation by TLR7–9. Nature 581, 316–322. 10.1038/s41586-020-2282-0. [PubMed: 32433612]
51. Krausgruber T, Blazek K, Smallie T, Alzabin S, Lockstone H, Sahgal N, Hussell T, Feldmann M, and Udalova IA (2011). IRF5 promotes inflammatory macrophage polarization and TH1-TH17 responses. Nat. Immunol. 12, 231–238. 10.1038/ni.1990. [PubMed: 21240265]
52. Saliba DG, Heger A, Eames HL, Oikonomopoulos S, Teixeira A, Blazek K, Androulidaki A, Wong D, Goh FG, Weiss M, et al. (2014). IR-F5:RelA Interaction Targets Inflammatory Genes in Macrophages. Cell Rep. 8, 1308–1317. 10.1016/j.celrep.2014.07.034. [PubMed: 25159141]
53. Lopez-Pelaez M, Lamont DJ, Peggie M, Shpiro N, Gray NS, and Cohen P (2014). Protein kinase IKKβ-catalyzed phosphorylation of IRF5 at Ser462 induces its dimerization and

nuclear translocation in myeloid cells. Proc. Natl. Acad. Sci. USA 111, 17432–17437. 10.1073/pnas.1418399111. [PubMed: 25326418]

54. Ren J, Chen X, and Chen ZJ (2014). IKKβ is an IRF5 kinase that instigates inflammation. Proc. Natl. Acad. Sci. USA 111, 17438–17443. 10.1073/pnas.1418516111. [PubMed: 25326420]
55. Stelzer S, Basso W, Benavides Silvá n J, Ortega-Mora LM, Maksimov P, Gethmann J, Conraths FJ, and Schares G (2019). Toxoplasma gondii infection and toxoplasmosis in farm animals: Risk factors and economic impact. Food Waterborne Parasitol. 15, e00037. 10.1016/j.fawpar.2019.e00037.
56. Dubey JP (1998). Advances in the life cycle of Toxoplasma gondii. Int. J. Parasitol. 28, 1019–1024. 10.1016/S0020-7519(98)00023-X. [PubMed: 9724872]
57. Koblansky AA, Jankovic D, Oh H, Hieny S, Sungnak W, Mathur R, Hayden MS, Akira S, Sher A, and Ghosh S (2013). Recognition of Profilin by Toll-like Receptor 12 Is Critical for Host Resistance to Toxoplasma gondii. Immunity 38, 119–130. 10.1016/j.immuni.2012.09.016. [PubMed: 23246311]
58. Wan Y, Xiao H, Affolter J, Kim TW, Bulek K, Chaudhuri S, Carlson D, Hamilton T, Mazumder B, Stark GR, et al. (2009). Interleukin-1 Receptor-associated Kinase 2 Is Critical for Lipopolysaccharide-mediated Post-transcriptional Control. J. Biol. Chem. 284, 10367–10375. 10.1074/jbc.M807822200. [PubMed: 19224918]
59. Muzio M, Ni J, Feng P, and Dixit VM (1997). IRAK (Pelle) Family Member IRAK-2 and MyD88 as Proximal Mediators of IL-1 Signaling. Science 278, 1612–1615. 10.1126/science.278.5343.1612. [PubMed: 9374458]
60. Wesche H, Gao X, Li X, Kirschning CJ, Stark GR, and Cao Z (1999). IRAK-M Is a Novel Member of the Pelle/Interleukin-1 Receptor-associated Kinase (IRAK) Family. J. Biol. Chem. 274, 19403–19410. 10.1074/jbc.274.27.19403. [PubMed: 10383454]
61. Zhou H, Bulek K, Li X, Herjan T, Yu M, Qian W, Wang H, Zhou G, Chen X, Yang H, et al. (2017). IRAK2 directs stimulus-dependent nuclear export of inflammatory mRNAs. Elife 6, e29630. 10.7554/eLife.29630.
62. Kanev GK, de Graaf C, Kooistra AJ, de Esch IJP, Leurs R, Wu€rdinger T, Westerman BA, and Kooistra AJ (2019). The Landscape of Atypical and Eukaryotic Protein Kinases. Trends Pharmacol. Sci. 40, 818–832. 10.1016/j.tips.2019.09.002. [PubMed: 31677919]
63. Mason NJ, Liou H-C, and Hunter CA (2004). T Cell-Intrinsic Expression of c-Rel Regulates Th1 Cell Responses Essential for Resistance to Toxoplasma gondii. J. Immunol. 172, 3704–3711. 10.4049/jimmunol.172.6.3704. [PubMed: 15004174]
64. Heng TSP, and Painter MW; Immunological Genome Project Consortium (2008). The Immunological Genome Project: networks of gene expression in immune cells. Nat. Immunol. 9, 1091–1094. 10.1038/ni1008-1091. [PubMed: 18800157]
65. Chang HR, Grau GE, and Pechè re JC (1990). Role of TNF and IL-1 in infections with Toxoplasma gondii. Immunology 69, 33–37. [PubMed: 2107144]
66. Sher A, Oswald IP, Hieny S, and Gazzinelli RT (1993). Toxoplasma gondii induces a T-independent IFN-gamma response in natural killer cells that requires both adherent accessory cells and tumor necrosis factor-alpha. J. Immunol. 150, 3982–3989. 10.4049/jimmunol.150.9.3982. [PubMed: 8473745]
67. Khan IA, Thomas SY, Moretto MM, Lee FS, Islam SA, Combe C, Schwartzman JD, and Luster AD (2006). CCR5 Is Essential for NK Cell Trafficking and Host Survival following Toxoplasma gondii Infection. PLoS Pathog. 2, e49. 10.1371/journal.ppat.0020049. [PubMed: 16789839]
68. Schoenemeyer A, Barnes BJ, Mancl ME, Latz E, Goutagny N, Pitha PM, Fitzgerald KA, and Golenbock DT (2005). The Interferon Regulatory Factor, IRF5, Is a Central Mediator of Toll-like Receptor 7 Signaling. J. Biol. Chem. 280, 17005–17012. 10.1074/jbc.M412584200. [PubMed: 15695821]
69. Keating SE, Maloney GM, Moran EM, and Bowie AG (2007). IRAK-2 participates in multiple Toll-like receptor signaling pathways to NFkB via activation of TRAF6 ubiquitination. J. Biol. Chem. 282, 33435–33443. 10.1074/jbc.M705266200. [PubMed: 17878161]

70. Balkhi MY, Fitzgerald KA, and Pitha PM (2008). Functional Regulation of MyD88-Activated Interferon Regulatory Factor 5 by K63-Linked Polyubiquitination. Mol. Cell Biol. 28, 7296–7308. 10.1128/MCB.00662-08. [PubMed: 18824541]

71. Zhang H, Bernaleau L, Delacrétaz M, Hasanovic E, Drobek A, Eibel H, and Rebsamen M (2023). SLC15A4 controls endolysosomal TLR7–9 responses by recruiting the innate immune adaptor TASL. Cell Rep. 42, 112916. 10.1016/j.celrep.2023.112916.

72. Chen Y, Lei X, Jiang Z, and Fitzgerald KA (2021). Cellular nucleic acid–binding protein is essential for type I interferon–mediated immunity to RNA virus infection. Proc. Natl. Acad. Sci. USA 118, e2100383118. 10.1073/pnas.2100383118.

73. Gazzinelli RT, and Denkers EY (2006). Protozoan encounters with Toll-like receptor signalling pathways: implications for host parasitism. Nat. Rev. Immunol. 6, 895–906. 10.1038/nri1978. [PubMed: 17110955]

74. Caetano BC, Carmo BB, Melo MB, Cerny A, dos Santos SL, Bartholomeu DC, Golenbock DT, and Gazzinelli RT (2011). Requirement of UNC93B1 Reveals a Critical Role for TLR7 in Host Resistance to Primary Infection with Trypanosoma cruzi. J. Immunol. 187, 1903–1911. 10.4049/jimmunol.1003911. [PubMed: 21753151]

75. Schamber-Reis BLF, Petritus PM, Caetano BC, Martinez ER, Okuda K, Golenbock D, Scott P, and Gazzinelli RT (2013). UNC93B1 and Nucleic Acid-sensing Toll-like Receptors Mediate Host Resistance to Infection with Leishmania major. J. Biol. Chem. 288, 7127–7136. 10.1074/jbc.M112.407684. [PubMed: 23325805]

76. de Boer J, Williams A, Skavdis G, Harker N, Coles M, Tolaini M, Norton T, Williams K, Roderick K, Potocnik AJ, and Kioussis D (2003). Transgenic mice with hematopoietic and lymphoid specific expression of Cre. Eur. J. Immunol. 33, 314–325. 10.1002/immu.200310005. [PubMed: 12548562]

77. Mach N, Gillessen S, Wilson SB, Sheehan C, Mihm M, and Dranoff G (2000). Differences in Dendritic Cells Stimulated in Vivo by Tumors Engineered to Secrete Granulocyte-Macrophage Colony-stimulating Factor or Flt3-Ligand1. Cancer Res. 60, 3239–3246. [PubMed: 10866317]

78. Lock JA (1953). Cultivation of Toxoplasma gondii in tissue culture in mammalian cells. Lancet 1, 324–325. 10.1016/S0140-6736(53)90996-9. [PubMed: 13012076]

79. Schneider CA, Rasband WS, and Eliceiri KW (2012). NIH Image to ImageJ: 25 years of image analysis. Nat. Methods 9, 671–675. 10.1038/nmeth.2089. [PubMed: 22930834]

Highlights

- IRAK1 and IRAK2 are redundant for IL-12 production upon *T. gondii* infection *in vivo*
- IL-12 production requires IRAK1 in DCs, while MO-DCs require IRAK2
- IRAK-mediated activation of IRF5 controls *Il12b* expression
- IRF5 binding to the *Il12b* promoter is enhanced by CNBP

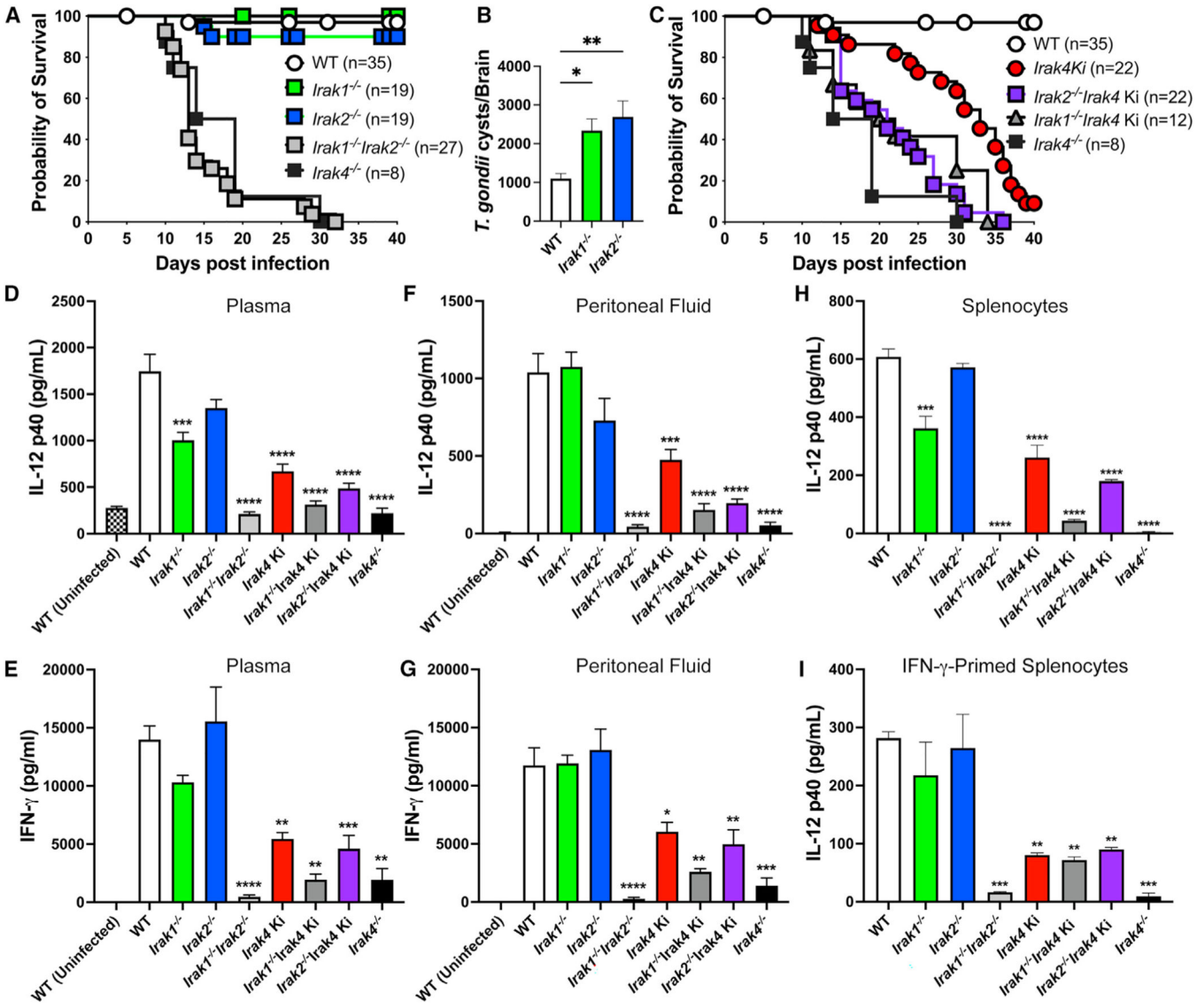

Figure 1. IRAKs control primary infection with *T. gondii*

(A and C) Survival data from C57BL/6 mice IP infected with *T. gondii* Me49 (25 cysts per mouse): WT (n = 35), *Irak1*$^{-/-}$ (n = 19), *Irak2*$^{-/-}$ (n = 19), *Irak1*$^{-/-}$*Irak2*$^{-/-}$ (n = 27), *Irak4* Ki (n = 22), *Irak1*$^{-/-}$*Irak4* Ki (n = 12), *Irak2*$^{-/-}$*Irak4* Ki (n = 22), and *Irak4*$^{-/-}$ (n = 8).

(B) Cysts counts in the brain of WT (n = 15), *Irak1*$^{-/-}$ (n = 14), and *Irak2*$^{-/-}$ (n = 13) mice IP infected with *T. gondii* Me49 (25 cysts per mouse) for 40 days.

(D–G) Quantification of IL-12 p40 and IFN-γ in the plasma (D and E) and peritoneal cavity (F and G) 5 days post IP infection with *T. gondii* Me49 (25 cysts per mouse) in WT (n = 13), *Irak1*$^{-/-}$ (n = 7), *Irak2*$^{-/-}$ (n = 14), *Irak1*$^{-/-}$*Irak2*$^{-/-}$ (n = 6), *Irak4* Ki (n = 12), *Irak1*$^{-/-}$*Irak4* Ki (n = 4), *Irak2*$^{-/-}$*Irak4* Ki (n = 14), and *Irak4*$^{-/-}$ (n = 5) mice or mice mock-infected with PBS (WT uninfected, n = 10).

(H and I) IL-12 p40 production in splenocytes unprimed (H) or primed with IFN-γ (100 ng mL^{-1}, 24 h) after *in vitro* infection with *T. gondii* Me49 tachyzoites at multiplicity of infection (MOI) 3 for 24 h (n = 2 for all strains). n represents the number of animals.

In (A) and (C), survival data were pooled from five independent experiments. In (B) and (D)–(I), data were pooled from two (H and I), three (B), or four (D–G) independent experiments and are presented as mean ± standard error of the mean (SEM). Each independent experiment consisted of three technical replicates. *$p < 0.05$, **$p < 0.01$, ***$p < 0.001$, ****$p < 0.0001$ in relation to the WT (one-way analysis of variance [ANOVA] with Tukey's multiple-comparisons test).

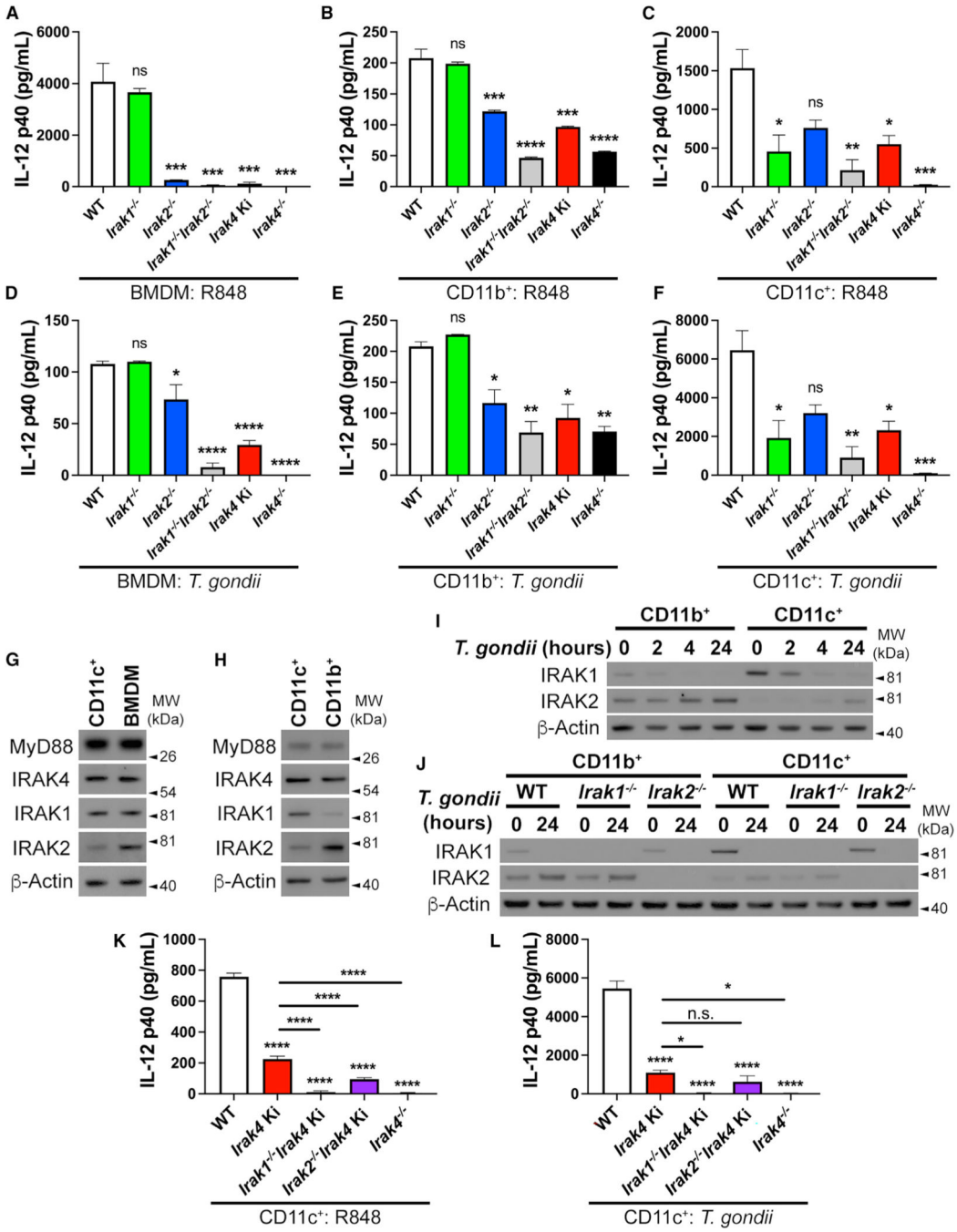

Figure 2. IRAK1 is required for IL-12 production in CD11c$^+$ DCs

(A–F) IL-12 p40 production by BMDMs (A and D), splenic CD11b$^+$ (B and E), and CD11c$^+$ DCs (C and F) treated with R848 (1 μg mL^{-1}, 24 h) (A–C) or exposed to *T. gondii* Me49 tachyzoites (MOI 3, 24 h) (D–F).

(G and H) Immunoblot of whole-cell lysates from CD11c$^+$ DCs, splenic CD11b$^+$ cells, and BMDMs.

(I) Immunoblot of phosphatase- and deubiquitinase-treated whole-cell lysates from splenic CD11b$^+$ and CD11c$^+$ DCs exposed to *T. gondii* Me49 tachyzoites (MOI 3) for up to 24 h.

(J) Immunoblot of phosphatase- and deubiquitinase-treated whole-cell lysates from splenic $CD11b^+$ and $CD11c^+$ DCs from the indicated strains exposed to *T. gondii* Me49 tachyzoites (MOI 3) for up to 24 h.

(K and L) IL-12 p40 production in $CD11c^+$ DCs of the indicated strains exposed to *T. gondii* Me49 tachyzoites (MOI 3, 24 h).

In (A)–(F), (K), and (L), data were pooled from three independent experiments and are presented as mean ± SEM; each independent experiment consisted of three technical replicates. Images are representative of three (G and H), four (J), or six (I) independent experiments. ns, not significant. *$p < 0.05$, **$p < 0.01$, ***$p < 0.001$, ****$p < 0.0001$ in relation to the WT (ANOVA with Tukey's multiple-comparisons test).

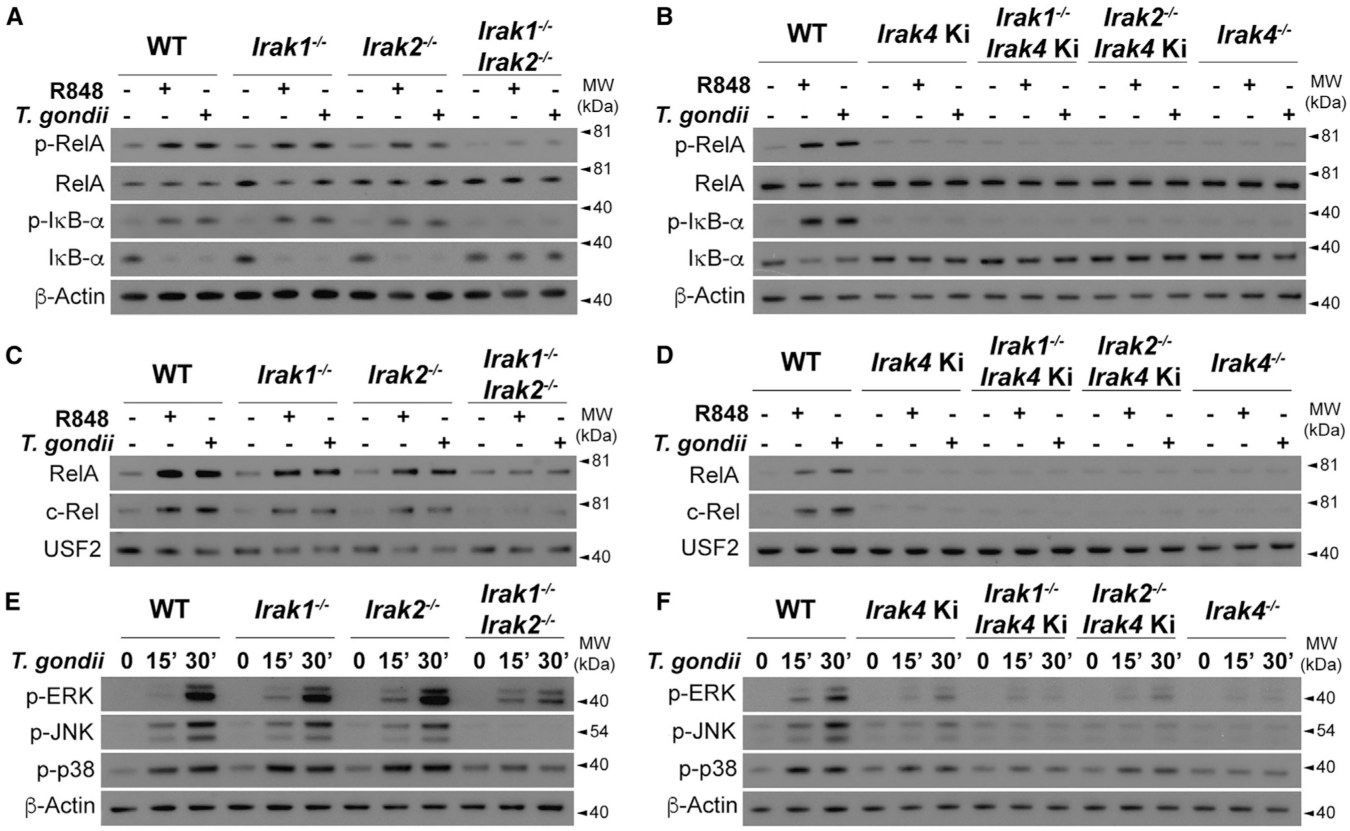

Figure 3. IRAK1 and IRAK2 are redundant for NF-κB and MAPK activation, while IRAK4 kinase activity is essential

(A–F) Immunoblot analysis of CD11c^{+} DCs of the indicated strains. Images are representative of three independent experiments.

(A and B) RelA phosphorylation, total RelA, IkB-a phosphorylation, and degradation in CD11c^{+} DCs treated with R848 (1 μg mL^{-1}, 30 min) or exposed to *T. gondii* Me49 tachyzoytes (MOI 3, 30 min).

(C and D) RelA and c-Rel in nuclear extracts of CD11c^{+} DCs exposed to *T. gondii* Me49 tachyzoites (MOI 3, 30 min).

(E and F) Phosphorylation of ERK, JNK, and p38 in CD11c^{+} DCs exposed to *T. gondii* Me49 tachyzoites (MOI 3, 15 and 30 min).

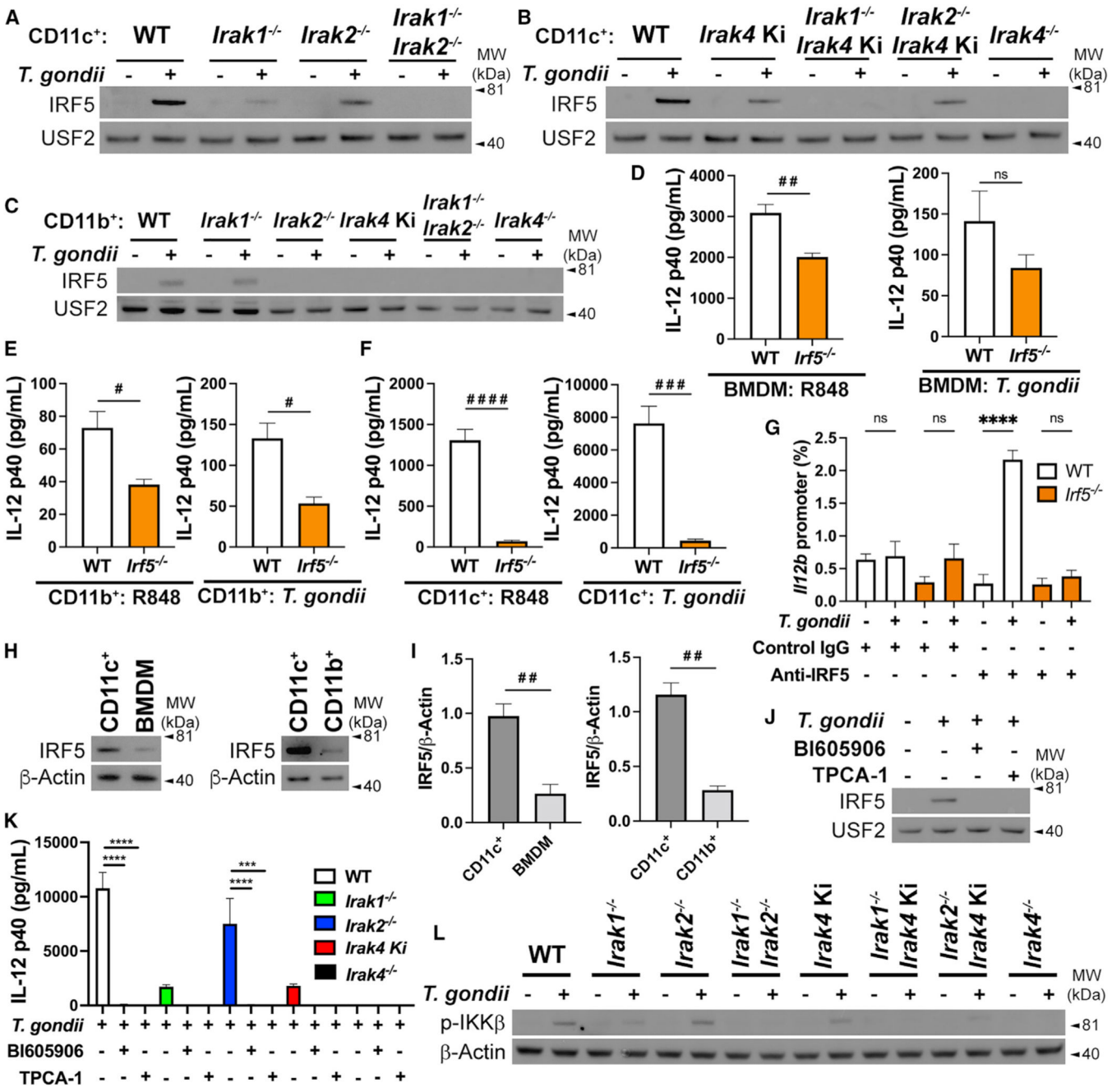

Figure 4. IL-12 production by CD11c$^+$ DCs is mediated by IRAK1 via IRF5

(A–C) IRF5 immunoblots from nuclear extracts of CD11c$^+$ DCs (A and B) or splenic CD11b$^+$ cells (C) infected with *T. gondii* Me49 tachyzoites (MOI 3, 2 h). (D–F) IL-12 p40 production in WT and *Irf5*$^{-/-}$ BMDMs (D), splenic CD11b$^+$ (E), and CD11c$^+$ DCs (F) treated with R848 (1 μg mL^{-1}, 24 h) or exposed to *T. gondii* Me49 tachyzoites (MOI 3, 24 h).

(G) ChIP-qPCR using control immunoglobulin G (IgG) or anti-IRF5 in WT and *Irf5*$^{-/-}$ CD11c$^+$ DCs, uninfected or infected with *T. gondii* Me49 tachyzoites (MOI 3, 2 h).

(H and I) IRF5 Immunoblot of whole-cell lysates from $CD11c^+$ DCs, splenic $CD11b^+$, and BMDMs (H) and densitometric quantifications (I).

(J) IRF5 immunoblots from nuclear extracts of $CD11c^+$ DCs infected with *T. gondii* Me49 tachyzoites (MOI 3, 2 h) with or without the IKKβ inhibitors BI605906 (10 μg mL^{-1}) or TPCA-1 (10 μg mL^{-1}).

(K) IL-12 p40 production by $CD11c^+$ DCs exposed to *T. gondii* Me49 tachyzoites (MOI 3, 24 h) with or without the IKKβ inhibitors BI605906 (10 μg mL^{-1}) or TPCA-1 (10 μg mL^{-1}).

(L) Immunoblot of *p*-IKKβ in whole-cell lysates of $CD11c^+$ DCs infected with *T. gondii* Me49 tachyzoites (MOI 3, 2 h).

Images are representative of two (C and J) or three (A, B, H, and L) independent experiments. In (D)–(G), (I), and (K), data were pooled from three independent experiments and are presented as mean ± SEM; each independent experiment consisted of three technical replicates. ***$p < 0.001$, ****$p < 0.0001$ (ANOVA with Tukey's multiple-comparisons test). #$p < 0.05$, ##$p < 0.01$, ###$p < 0.001$ (unpaired t test).

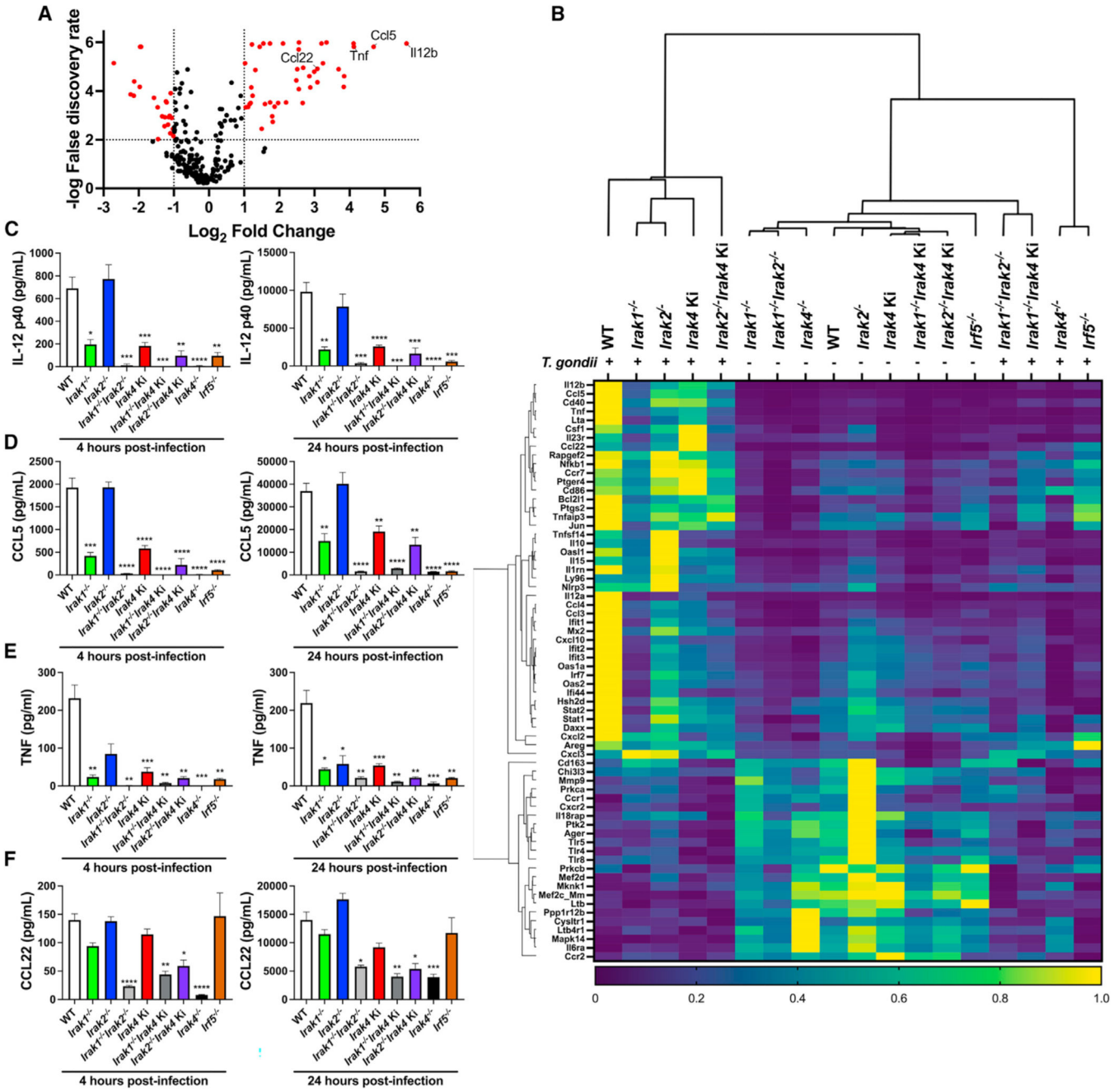

Figure 5. Production of inflammatory cytokines and chemokines by DCs requires IRAK1, IRAK4, and IRF5

(A) Volcano plot depicting *T. gondii*-infected versus uninfected CD11c$^+$ DCs (WT). The horizontal dashed line represents a —log false discovery rate of 2, and the vertical dashed lines represent a $\log_2$ fold change of −1 and +1.

(B) Heatmap showing the expression and hierarchical clustering of selected genes in CD11c$^+$ DCs from the indicated strains, uninfected or infected with *T. gondii* Me49 tachyzoites (MOI 3, 4 h).

(C–F) Quantification of IL-12 p40 (C), CCL5 (D), TNF (E), and CCL22 (F) in culture supernatants of $CD11c^+$ DCs of the indicated strains infected with *T. gondii* Me49 (MOI 3) for 4 and 24 h.

In (A) and (B), Data were pooled from four independent experiments. In (C)–(F), data were pooled from four independent experiments and are presented as mean ± SEM; each independent experiment consisted of one technical replicate. *$p < 0.05$, **$p < 0.01$, ***$p < 0.001$, ****$p < 0.0001$ (ANOVA with Tukey's multiple-comparisons test).

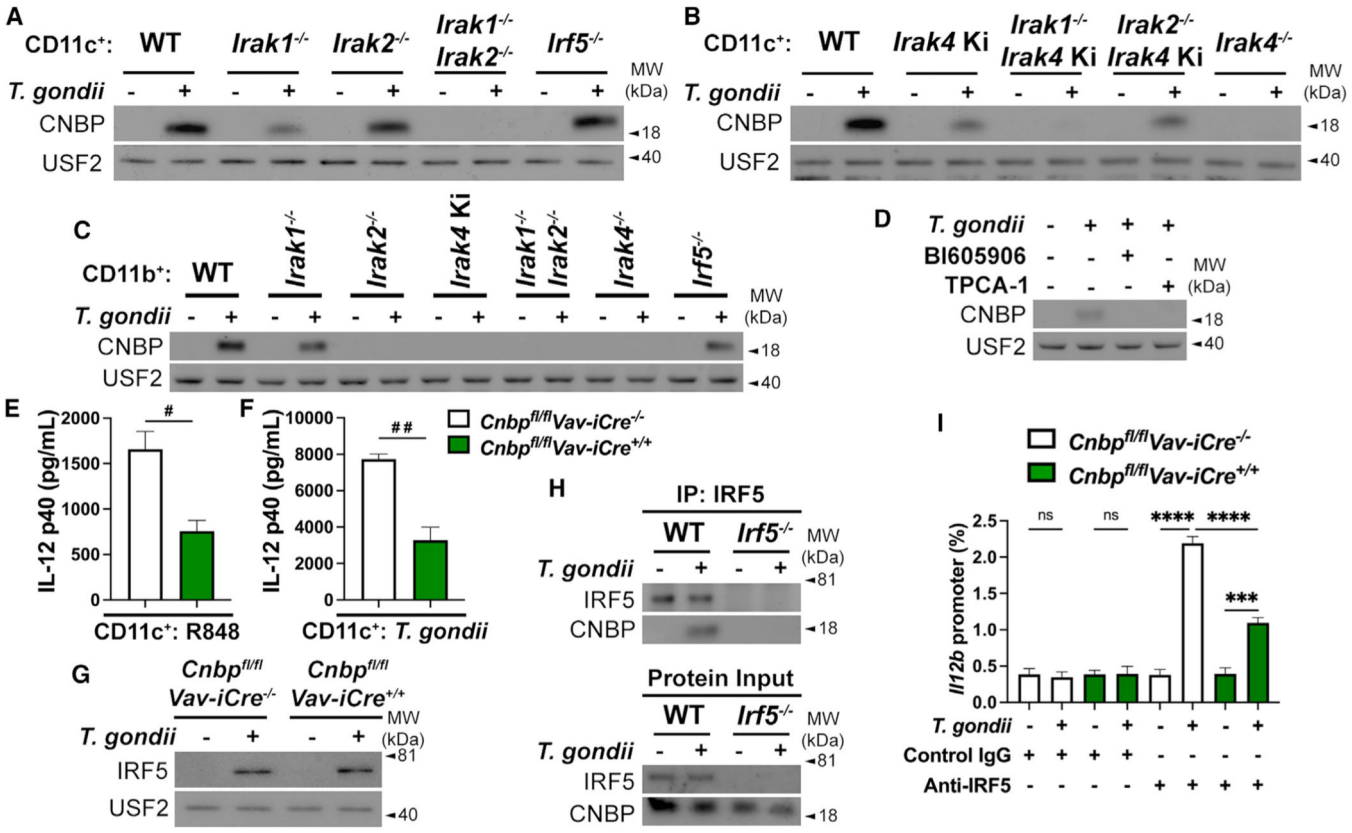

Figure 6. IRAK1-mediated CNBP activation enhances IL-12 production in CD11c$^+$ DCs

(A–C) CNBP nuclear translocation in CD11c$^+$ DCs (A and B) and splenic CD11b$^+$ cells (C) infected with *T. gondii* Me49 tachyzoites (MOI 3, 2 h).

(D) CNBP nuclear translocation in CD11c$^+$ DCs infected with *T. gondii* Me49 tachyzoites (MOI 3, 2 h) with or without the IKKβ inhibitors BI605906 (10 μg mL^{-1}) or TPCA-1 (10 μg mL^{-1}).

(E and F) IL-12 p40 production in *Cnbp$^{fl/fl}$Vav-iCre$^{-/-}$* and *Cnbp$^{fl/fl}$Vav-iCre$^{+/+}$* CD11c$^+$ DCs stimulated with R848 (1 μg mL^{-1}, 24 h) (E) or *T. gondii* Me49 tachyzoites (MOI 3, 24 h) (F).

(G) IRF5 nuclear translocation in *Cnbp$^{fl/fl}$Vav-iCre$^{-/-}$* and *Cnbp$^{fl/fl}$Vav-iCre$^{+/+}$* CD11c$^+$ DCs exposed to *T. gondii* Me49 tachyzoites (MOI 3, 2 h).

(H) IRF5 and CNBP co-immunoprecipitation in WT and *Irf5$^{-/-}$* CD11c$^+$ DCs exposed to *T. gondii* Me49 tachyzoites (MOI 3, 2 h).

(I) ChIP-qPCR using control IgG or anti-IRF5 in *Cnbp$^{fl/fl}$Vav-iCre$^{-/-}$* and *Cnbp$^{fl/fl}$Vav-iCre$^{+/+}$* CD11c$^+$ DCs, uninfected or infected with *T. gondii* Me49 tachyzoites (MOI 3, 2 h).

Images are representative of two (C and D) or three (A, B, G, and H) independent experiments. In (E), (F), and (I), data were pooled from three independent experiments and are presented as mean ± SEM; each independent experiment consisted of three technical replicates. ***p < 0.001, ****p < 0.0001 (ANOVA with Tukey's multiple-comparisons test). #p < 0.05, ##p < 0.01, ###p < 0.001 (unpaired t test).

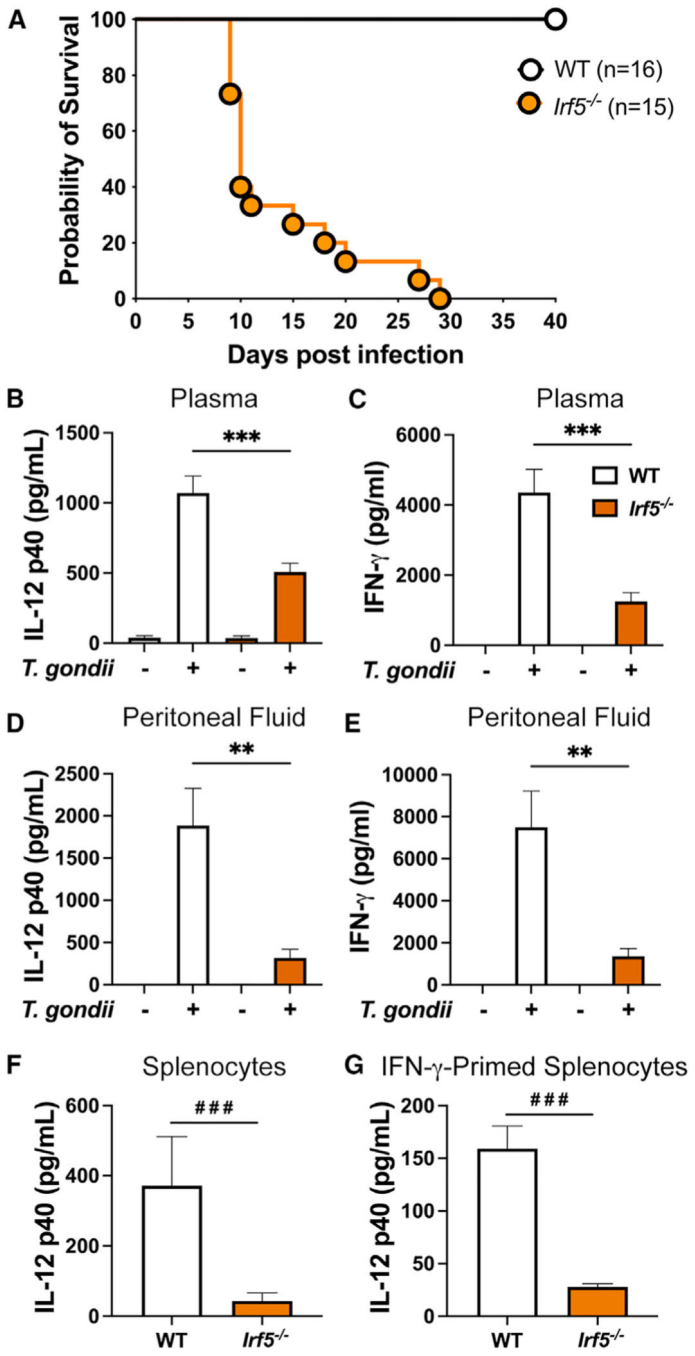

Figure 7. IRF5 controls primary infection with *T. gondii*

(A) Survival data from C57BL/6 WT (n = 16) and *Irf5*$^{-/-}$ (n = 15) mice IP infected with *T. gondii* Me49 (25 cysts per mouse).

(B–E) Quantification of IL-12 p40 and IFN-γ in the plasma (B and C) and peritoneal cavity (D and E) in WT (n = 14) and *Irf5*$^{-/-}$ (n = 12) mice 5 days post IP infection with *T. gondii* Me49 (25 cysts per mouse) or mock infected with PBS WT (n = 4) and *Irf5*$^{-/-}$ (n = 3) (uninfected controls).

(F and G) IL-12 p40 production in splenocytes unprimed (n = 5 for each strain) (F) or primed with IFN-γ (100 ng mL^{-1}, 24 h) (n = 3 for each strain) (G) after *in vitro* infection with *T. gondii* Me49 tachyzoites at MOI 3 for 24 h n represents the number of animals. In (A), survival data were pooled from two independent experiments. In (B)–(G), data were pooled from three independent experiments and are presented as mean ± SEM; each independent experiment consisted of three technical replicates. *p < 0.05, **p < 0.01, ***p < 0.001, ****p < 0.0001 in relation to the WT (ANOVA with Tukey's multiple-comparisons test). ###p < 0.001 (unpaired t test).

KEY RESOURCES TABLE

REAGENT or RESOURCE	SOURCE	IDENTIFIER
Antibodies		
Rabbit mAb anti-IRAK1 (D51G7)	Cell Signaling	4504S; RRID AB_1904032
Rabbit pAb anti-IRAK2	Abcam	ab62419; RRID AB_956084
Rabbit pAb anti-IRAK4	Novus	NB500–597; RRID AB_2943026
Goat pAb anti-MyD88	R&D Systems	AF3109; RRID AB_2146703
Rabbit pAb anti-IRF5	Cell Signaling	4950; RRID AB_836887
Rabbit pAb anti-USF2	Novus Biologicals	NBP1–92649; RRID AB_11007053
Rabbit mAb anti-*c*-Rel (D3B8S)	Cell Signaling	67489; RRID AB_2799726
Rabbit mAb anti-phospho-IkBa (Ser32) (14D4)	Cell Signaling	2859; RRID AB_561111
Rabbit mAb anti-phospho-NF-kB p65 (Ser 536) (93H1)	Cell Signaling	3033; RRID AB_331284
Rabbit pAb anti-Actin	Sigma-Aldrich	A2066; RRID AB_476693
Rabbit mAb anti-IkB-a (44D4)	Cell Signaling	4812S; RRID AB_10694416
Rabbit pAb anti-RelA/NF-kB p65	Novus Biologicals	NB100–2176; RRID AB_535932
Rabbit pAb anti-Goat-IgG HRP-conjugated	R&D Systems	HAF017; RRID AB_562588
Horse pAb anti-Mouse-IgG HRP-conjugated	Cell Signaling	7076; RRID AB_330924
Goat pAb anti-Rabbit IgG (whole molecule) Peroxidase	Sigma-Aldrich	A0545; RRID AB_257896
Rabbit mAb anti-phospho-SAPK/JNK MAPK (81E11)	Cell Signaling	4668T; RRID AB_823588
Rabbit mAb anti-phospho-p38 MAPK (D3F9)	Cell Signaling	4511T; RRID AB_2139682
Rabbit mAb anti-phospho-p44/42 (Erk1/2) (D13.14.4E)	Cell Signaling	4370T; RRID AB_2315112
Rabbit mAb anti-phospho-IKK	Cell Signaling	2697T; RRID AB_2079382
Mouse mAb anti-CNBP (H-7)	Santa Cruz	sc-515387-X; AB_2943027
Rat mAb anti-mouse CD16/32	BioLegend	101301; RRID AB_312800
F4/80 (clone BM8) PE-Cy5	BioLegend	123112; RRID: AB_893482
CD11b (clone M1/70) PE-Cy7	BioLegend	101216; RRID: AB_312799
DCSign (clone MMD3) eFluor660	Thermo Fisher	15361890; RRID: 11219065
MHCII (clone AF6–120.1) PE	BioLegend	116408; RRID: 313727
Chemicals, peptides, and recombinant proteins		
ACK Lysing Buffer	Gibco	A1049201

REAGENT or RESOURCE	SOURCE	IDENTIFIER
BI605906	Millipore-Sigma	SML3370
Blotting-Grade Blocker	Bio-Rad	1706404
Dithiothreitol (DTT, Cleland's Reagent)	Boston Bioproducts	#P-765–10G
Dulbecco's Modification of Eagle's Medium	Corning	10–013-CV
Dulbecco's Phosphate-Buffered Saline	Corning	21–031-CV
Ethylenediamine tetraacetic acid (EDTA)	Boston Bioproducts	BM-150
Fetal Bovine Serum - Premium	R&D Systems	S11150
Glycerol	Fisher Scientific	BP229
Halt Phosphatase Inhibitor Cocktail (100x)	Thermo-Fisher	1862495
Halt Protease Inhibitor Cocktail (100x)	Thermo-Fisher	87786
HEPES	Thermo-Fisher	15630106
Interferon-Gamma, Recombinant	BioLegend	575308
L-Glutamine	Gibco	25030–081
Lambda protein phosphatase	Millipore-Sigma	P9614
Live/Dead Ghost Aqua V510	Tonbo Biosciences	13–0870-T100
NaF	Sigma-Aldrich	201154
NaVO4	Sigma-Aldrich	567540
NP-40 (Nonidet P-40 Substitute)	Boston Bioproducts	#P-877
Penicilin Streptomycin Solution, 100x	Corning	30–002-CI
Pierce™ Lane Marker Reducing Sample Buffer	Thermo-Fisher	39000
Protein G Sepharose 4 Fast Flow	Millipore Sigma	GE17–0618-01
R848 (Resiquimod)	Invivogen	tlrl-r848
Recombinant Human USP2	R&D	E—504–050
Sodium Chloride	Sigma-Aldrich	S5886
TMB Substrate Reagent Set	BD	555214
TPCA-1	Cell Signaling	50902
Tris hydrochloride	Roche	10812846001
Tween 20	Boston Bioproducts	#P-934
β-Glycerophosphate disodium	Santa Cruz	sc-203323
Critical commercial assays		

REAGENT or RESOURCE	SOURCE	IDENTIFIER
CD11b microbeads, human and mouse	Miltenyi Biotec	130–097-142
CD11c microbeads, mouse	Miltenyi Biotec	130–125-835
Clarity Max Western ECL Substrate	Bio-Rad	1705062
NE-Per™ Nuclear and Cytoplasmic Extraction Reagents	Thermo-Fisher	78833
IL-12/IL-23 p40 (Total) Mouse Uncoated ELISA Kit	Invitrogen	88–7120-88
Mouse CCL5/RANTES DuoSet ELISA	R&D Systems	DY478
Mouse CCL22 DuoSet ELISA	R&D Systems	DY439
Mouse IFN-gamma DuoSet ELISA	R&D Systems	DY485
Mouse TNF-alpha DuoSet ELISA	R&D Systems	DY410
nCounter Mouse Inflammation V2 Panel	Nanostring	XT-CSO-MIN2–12
Deposited data		
Mendeley data	This paper	https://doi.org/10.17632/4z4pk9rxb3.1
Experimental models: Organisms/strains		
C57/BL6 - WT	The Jackson Laboratory	000664
C57/BL6 - *Irak1*$^{-/-}$	The Jackson Laboratory	031842
C57/BL6 - *Irak2*$^{-/-}$	The Jackson Laboratory	031916
C57/BL6 - *Irak1*$^{-/-}$ *Irak2*$^{-/-}$	This paper	NA
C57/BL6 - *Irak4*$^{-/-}$	Suzuki et al.[29]	NA
C57/BL6 - *Irak4* Ki	Tae et al.[37]	NA
C57/BL6 - *Irak1*$^{-/-}$ *Irak4* Ki	This paper	NA
C57/BL6 - *Irak2*$^{-/-}$ *Irak4* Ki	This paper	NA
C57/BL6 - *Irf5*$^{-/-}$	Takaoka et al.[47]	NA
C57/BL6 - *Vav-i*Cre	The Jackson Laboratory	008610
C57/BL6 - *Vav-i*Cre *Cnbp*$^{fl/fl}$	Chen et al.[72]	NA
Toxoplasma gondii strain me49	ATCC	ATCC 50611
Oligonucleotides		
Il12b ISRE - Fwd	Takaoka et al.[47]	5’-ACCCCGAAGTCATTTCCTCT-3’

REAGENT or RESOURCE	SOURCE	IDENTIFIER
Il12b ISRE - Rev	Takaoka et al.[47]	5' -ACCCACTGTTCCTTCTGCT-3'
Software and algorithms		
GraphPad Prism	Graphpad Software	www.graphpad.com
FlowJo	BD	www.flowjo.com
ImageJ	NIH	ImageJ.nih.gov/ij/